



**Premature Deterioration in Michigan
Jointed Concrete Pavements on Open
Graded Drainage Courses**

Draft Final Report
to the

Michigan Department of Transportation

LAST COPY
DO NOT REMOVE FROM LIBRARY

**Department of Civil and
Environmental Engineering**

The University of Michigan
College of Engineering

Ann Arbor, MI 48109-2125

TESTING AND RESEARCH SECTION
CONSTRUCTION AND TECHNOLOGY DIVISION
RESEARCH REPORT NO. RC-1456

DRAFT

**Premature Deterioration in Michigan
Jointed Concrete Pavements on Open
Graded Drainage Courses**

Draft Final Report
to the

Michigan Department of Transportation

By

Dr. Will Hansen, Associate Professor
Department of Civil and Environmental Engineering
University of Michigan, Ann Arbor (U of M)

Dr. Thomas J. Van Dam, Assistant Professor
Department of Civil Engineering
Michigan Technological University (MTU)

Participating Researchers at U of M:

Chris Byrum, Andrew Definis, Gail Grove, Elin Jensen,
Ashraf Mohamed, Phil Mohr, and Ivindra Pane

Participating Researchers at MTU:

Matthew Wachholz

November 11, 1997

Acknowledgments

The research described in this project was sponsored by the Michigan Department of Transportation (MDOT). The authors wish to extend their sincere appreciation and thanks to John Staton, Chair of Technical Advisory Group (TAG) for his support and cooperation throughout this project. Additionally, the author wishes to thank the entire TAG for their support and guidance. The authors also thank Dr. Thomas J. Van Dam of the Michigan Technological University for conducting the literature review, resilient modulus testing, and American Association of State Highway and Transportation Officials (AASHTO) serviceability check.

Several graduate students from the Materials and Geotechnical divisions of the Department of Civil and Environmental Engineering at the University of Michigan participated in this research. The authors extend their special thanks to Andrew DeFinis, Elin Jensen, Phil Mohr, Ivindra Pane, Chris Byrum, Jonathan Galow, Kyle Ramakers, Aaron Berkholz and Dr. Ashraf Mohamed for their support in field and laboratory testing and in the preparation of this report. Additionally, a sincere thanks is extended to Matt Wachholz who helped with the study at Michigan Technological University.

This project could not have been carried out without the cooperation and help of many of the officials at the Michigan Department of Transportation (MDOT). Our sincere thanks are to Dave Smiley, Kurt Bancroft, Vern Barnhart, Dennis Dodson, Bob Kelly, Connie Houk, and Dawn Langlois. Dave Smiley provided the research team with valuable information and guidance. This research benefited from the expertise of the Falling Weight Deflectometer (FWD) crew and coring crew, led by Kurt Bancroft and Bob Kelly. Connie Houk, Dawn Langlois and Dennis Dodson provided the research team with valuable Pavement Management System (PMS) data.

The authors also wish to thank Dr. Starr Kohn of the Soil and Materials Engineers, Inc. (SME) for generously loaning a Dynamic Cone Penetrometer (DCP) to the research team when needed.

Table of Contents

Acknowledgement.....
1. Introduction and Problem Statement.....	1
1.1 Overview and Background.....	1
1.2 Problem Statement.....	3
1.3 About This Report.....	3
2. Research Objectives and Scope of Work.....	7
2.1 Project Objectives.....	7
2.2 Scope of Work.....	7
3. Project Literature Review.....	9
3.1 Historical Perspective on OGDC Materials.....	10
3.2 Components of Drainage Pavement Systems.....	11
3.3 Performance of Jointed Concrete Pavements.....	13
3.3.1 The Pavement Environment and Key Mechanisms at Work.....	13
3.3.2 Moisture Related Effects on Distress Development.....	15
3.3.3 Apparent Effects of Base Type and Drainage System on Pavement Performance.....	17
3.3.4 Other Important Factors Affecting Transverse Cracking of Jointed Concrete Pavements.....	21
4. Experimental Design.....	24
4.1 Selection of Test Sections.....	24
4.1.1 PMS.....	26
4.1.2 RQI.....	27
4.1.3 Historical Records.....	29
4.1.4 Field Condition Survey.....	29
4.2 Field Testing.....	30
4.2.1 Site Photos.....	31
4.2.2 Distress and Damage Surveys and Crack Width Measurement.....	31
4.2.3 Concrete Coring.....	32
4.2.4 DCP Testing.....	32
4.2.5 Soil Sampling.....	33
4.2.6 FWD Testing.....	34
4.3 Laboratory Testing.....	34
4.3.1 Concrete Properties.....	34
4.3.2 Gradation- Loss on Wash and Sieve Analysis.....	35
4.3.3 Filter Criteria, Hazen Permeability.....	35
4.4 Resilient Modulus Laboratory Procedure.....	35

5. Study of Resilient Modulus and AASHTO Serviceability for OGDC Pavement Systems.....	40
5.1 Resilient Modulus Study on Two OGDC and Materials and One DGBC Material.....	40
5.2 Effect of Drainage on AASHTO Rigid Pavement Thickness Design.....	49
5.2.1 The AASHTO Thickness Design Procedure.....	49
5.2.2 Evaluation of the Effect of Drainage on Pavement Design Life.....	52
6. Analysis of Test Sections.....	57
6.1 Evaluation of Michigan Pavement Distress Levels With Respect to the LTPP Database	57
6.2 Major Causes for the Deterioration of the Michigan Study Sections.....	60
6.2.1 Drainage Issues.....	60
6.2.2 Slab Rocking and Thermal Effects.....	62
6.2.3 Crack Spalling.....	65
6.3 RQI as Measure of OGDC vs. DGBC Pavement Distress Development.....	65
7. Conclusion and Recommendations.....	68
8. References.....	69

Appendices

- A. OGDC Sections in Michigan
- B. Section Summaries and Control Section Logs
- C. Pavement Distress
- D. Selected Site Photos
- E. Construction Records
- F. Pavement Management System (PMS) and RQI (Ride Quality Index) Data
- G. Concrete Properties
- H. Foundation Properties
- H. Dynamic Cone Penetrometer (DCP) Data
- I. Falling Weight Deflectometer (FWD) Data

1. INTRODUCTION

1.1 Overview and Background

In the early to mid 1980's the Michigan Department of Transportation changed the standard specifications for materials used for base courses in the typical jointed reinforced concrete pavements. Prior to this period the standard base material was described as Dense Graded Base Course (DGBC). The new material has been defined as Open Graded Drainage Course (OGDC). Table 1.1 shows MDOT's use of OGDC materials by year since 1980. A complete listing of all MDOT projects with OGDC bases is found in Appendix A, including number of lane miles, where they are located, and when they were constructed.

In the early days of road building, DGBC was used exclusively. The concept being that the primary function of the base is to provide stability and support for the PCC pavement. The intent here is to use a particle size gradation which, upon compaction, results in a very low void ratio, dense layer. One belief is that the resulting lower void ratio and generally higher fines content of dense graded aggregates result in higher moisture contents along the bottoms of slabs and reduces the drainability of the pavement system considerably. Many types of distress such as D-cracking, ASR, pumping and frost heave related faulting and cracking, and more are known to require water as an essential ingredient for initiation and development.

In response to apparent drainability concerns, a second perspective as to the base's primary function came into being; namely that the base should allow all moisture that finds its way to the bottom of the PCC slab to drain away as rapidly as possible. This perspective lead to the use of OGDC gradations.

Various OGDC gradations have been experimented with in Michigan, starting about 1980. In mid-1980, a job specific Special Provision allowed the use of what are termed 6A modified, 9A, or 17A modified gradations. These gradations were 100% crushed and possibly treated with asphalt cement. Later that year, the 100% crushed requirement was reduced to 90% where the asphalt treatment was required.

In 1982, a new peastone OGDC gradation was added. The previous gradation for OGDC was revised from: 0-30% passing the #4 sieve and 0-5% passing the #8 sieve to: 0-8% passing the #4 sieve. This eliminated the finer side of the previous gradation. The LA Abrasion value was limited to 50 maximum.

During early 1983, the OGDC gradations were named 5G, 8G (based upon a modified 21AA standard dense graded aggregate, or the PennDOT OGS gradations), and 34G. Each of these gradations were fine tuned on certain individual sieves and percent crushed to solve problems encountered from one project to the next. The 8G was kept as drainable as possible by not allowing either the asphalt or portland cement coatings.

In 1984, MDOT adopted an open graded drainage course as the standard base to be used under their pavements. The 1984 Standard Specifications For Construction was the first time OGDC gradations (5G, 8G, and 34G) appeared in the MDOT Standard Specifications to be used for bases and underdrains. Through the rest of the 1980's these gradations remained essentially the same. By the time the 1990 Standard Specifications were distributed, a new 3G for bicycle paths and a 34R for underdrains were added to the book. During the early 1990's, the open graded gradations have had small changes, including requirements on construction practices. In particular, several versions of 3G Modified were experimented with in an attempt to increase stability and pavement support without sacrificing too much drainability.

The 1996 Standard Specifications list four OGDC gradations: 2G, 3G, 5G, and 34R. The 2G is a new name for one of the 3G Modifieds mentioned earlier, while the 8G and the 34G were dropped. The 3G is used as an unstabilized OGDC. The 2G is similar to 3G except that 2G is coarser on the #8 and #30 sieves and is treated with either asphalt or portland cement. The 2G option uses 100mm underdrain pipe for asphalt stabilization while 150mm pipe is required with the cement treated gradation. Specific construction practice differences for 2G versus the 3G are covered in Section 303 of the 1996 Standard Specifications. A new gradation being tried, 350AA (modified 21AA), is intended to be between the OGDC and DGBC gradations. Figure 1.1 shows the gradation bands for the current aggregates.

The sources of all OGDC gradations are allowed to consist of natural aggregates, iron blast-furnace slag, or reverberatory-furnace slag meeting the grading and physical requirements of Tables 902-1 & 902-2, respectively in the 1996 Standard Specifications. The LA Abrasion was changed to 45 for the present gradations and the percent crushed requirement has become more thoroughly defined in the 1996 book.

In order to evaluate the effect of OGDC on the performance of PCC pavements in Michigan, several test sections were reviewed in detail considering the effects of the following interacting variables:

1. *Concrete*: compressive strength, split tensile strength, elastic modulus
2. *Drainage system*: with or without edge drain, condition of drainage structure
3. *Shoulders*: shoulder type and intermediate joint design
4. *Base material*: OGDC, DGBC, type and gradation of aggregate, drainability.
5. *Subbase condition*: gradation, drainability.
6. *Traffic conditions and loading*
7. *Paving conditions*: temperature, humidity, time of year, curing of PCC, how soon construction and regular traffic allowed on.
8. *Pavement*: slab geometry and thickness

1.2 Problem Statement

Approximately 10 % of the projects that have been constructed with the new OGDC materials have been developing various distresses at relatively high rates over time. The distresses observed have typically consisted of premature transverse cracking, and slightly accelerated faulting and spalling. This premature development of distress has resulted in the initiation of this study to investigate the factors which may be causing them.

1.3 About This Report

Chapter 2 of this report summarizes the project objectives and scope of work. Chapter 3 summarizes the key points from an extensive literature review which was conducted in the beginning of the project. This review was used to guide the research and get an understanding of how Michigan fits in with the rest of the country on OGDC issues. This section also covers the rationale behind the use of open grade OGDC type materials, factors affecting distress development, drainage issues, and design issues related to concrete pavements.

Chapter 4 covers the components of the experiment conducted. As part of this study, field investigation was conducted on 14 pavement sections. The intent was to develop a database of information which would aid the researchers in quantifying relevant trends with respect to performance levels and distresses. The rationale behind the selection of the test sites is discussed. A detailed laboratory testing program on samples obtained from the field was also conducted. Procedures used in the development of the project database and methods used for analysis of the resulting data are discussed.

Chapter 5 discusses the results of a laboratory study on the resilient modulus testing of several OGDC materials and one DGBC material. In addition, the importance of drainage on AASHTO serviceability was evaluated in a sensitivity study.

Chapter 6 gives a detailed description of the causes of distress the tested sections, based on field and laboratory evaluations. In addition, the role of base course in OGDC pavement deterioration is discussed. A comparison of the Michigan test sections to the national LTPP database of pavement sections from similar environments is also presented.

Chapter 7 discusses the project conclusions and summarizes the work. The apparent role of OGDC in the big picture of pavement performance is discussed.

Finally, Chapter 8 contains the project reference list. A large number of appendices are included in a separate volume for this study. The mountain of compiled data, distress plots, photo logs from field testing, and laboratory testing results are contained within the various appendices.

Table 1.1 Summary of OGDC Construction in Michigan by year.

Year of Construction	Lane Miles Constructed
1980	1.932
1981	0.000
1982	0.160
1983	22.073
1984	112.979
1985	38.536
1986	92.463
1987	68.924
1988	52.360
1989	38.072
1990	49.143
1991	45.661
1992	39.389
1993	32.987
1994	10.389
1995	44.911
1996	0.000 N/A
1997	0.000 N/A
Total miles of OGDC	649.979

Table 902-1 Grading Requirements for Coarse Aggregates, Dense-Graded Aggregates, and Open-Graded Aggregates 1996

Material Type	Class	Item of Work by Section Number (Sequential) (a)	Sieve Analysis (b) (MTM 109) Total Percent Passing									Loss by Washing (b) (MTM 108) Percent 0.075 mm
			50 mm	37.5 mm	25.0 mm	19.0 mm	12.5 mm	9.5 mm	4.75 mm	2.36 mm	0.60 mm	
Coarse Aggregates	4 AA		100	90-100	20-55	0-15		0-5				1.5 max.
	6 AAA			100	95-100	60-85	30-60		0-8			1.0 max.(c)
	6 AA	601,603,706,708,806		100	95-100		30-60		0-8			1.0 max.(c)
	6 A	205,401,402,601,706,806										
	17 A				100	90-100	50-75		0-8			1.0 max.(c)
	26 A	706,712				100	95-100	60-90	5-30	0-12		3.0 max.
	29 A	506					100	90-100	10-30	0-10		3.0 max.
Dense-Graded Aggregates	21 AA	302,503		100	85-100		50-75			20-45		4-8(d)(f)
	21 A	302,503										
	22 A	302,306,307,503			100	90-100		65-85		30-50		4-8(d)(e)(f)
	23 A	306,307			100			60-85		25-60		9-16(f)
Open-Graded Aggregates	2 G	303(g)		100	85-100		40-70			0-10	0-8	5.0 max.
	3 G	303,304		100	85-100		40-70			0-30	0-13	5.0 max.
	5 G	205		100			0-90		0-8			3.0 max.
	34 R	404					100	90-100		0-5		3.0 max.

Figure 1.1 Specification Ranges for Concrete Pavement Bases in Michigan.

2. PROJECT OBJECTIVES AND SCOPE OF WORK

2.1 Project Objectives

The project objectives have evolved slightly over time since the inception of this project. The resulting project objectives, as modified from the original proposal, are as follows:

- To analyze in detail the structural and serviceability performance characteristics of relatively new pavements in Michigan. Specifically, to identify sections constructed on OGDC which have either performed relatively poorly or well and compare them to similar DGBC sections, attempting to identify key trends and differences in behavior.

KSJ - (•) To identify if OGDC is playing a significant role in the types of premature distresses observed.

- • To identify any other factors which may be responsible for observed premature deterioration at the selected test sites.

To find ways of identifying sections which are deteriorating.

- To provide recommendations as to future work and methods to improve performance of the next generation of concrete pavements in Michigan.

2.2 Scope of Work

The scope of work as outlined in the original proposal has also evolved since the inception of the projects as the research progressed. An outline of the work conducted is as follows:

Phase 1: Identification of performance and behavioral trends in OGDC and DGBC sections.

1. Obtain PMS Summary data for all OGDC sections placed in the recent past. Specifically review the data in terms of transverse cracking and spalling as a function of time and control section or construction contract.
2. Obtain PMS Summary data for all DGBC sections placed in the recent past. Specifically review the data in terms of transverse cracking and spalling as a function of time and control section or construction contract.
3. Obtain Ride Quality Index (RQI) data on the sections from above and track trends as a function of time and control section or construction contract.

4. Obtain traffic data and identify sections which have performed relatively poorly or well.
5. Identify the sections to be studied in detail by reviewing data from above and working with MDOT personnel.
6. Detailed structural and serviceability evaluation consisting of:
 - A. Distress and drainage surveys, mapping and quantifying observed distresses and notable feature
 - B. FWD testing on most study sections. The testing was done at mid-slab, corners, and edges at morning, noon, and mid afternoon times.
 - C. DCP testing at all test sections with the U.S. Army Corps. of Engineers device.
 - D. Core samples of the pavement were obtained for laboratory analysis.
 - E. Samples of base, subbase, and subgrade/embankment layers were obtained for laboratory analysis
7. Evaluate all above data prepare phase 1 report and recommend direction for phase 2.

Phase II: Identification of OGDC and Other Factors Responsible for Observed Premature Distresses

1. Review of historical records for environmental conditions during placement for the selected test sites.
2. Investigation of sections which exhibit transverse cracking very early in their design lives.
3. Determination of primary factors causing premature distresses observed.
4. Preparation of final report for the project.

3. PROJECT LITERATURE REVIEW

3.1 Historical Perspective on OGDC Materials

Since the construction of the first pavements, it has been noted that the presence of free water was detrimental to pavement performance. The ancient Romans (approximately 300 B.C.) mitigated the impact of water by constructing roads above the surrounding terrain, placing them on thick subbases of sand prior to cementing large rocks together to form the surface. Some of these roads are still in use today, roughly 2,300 years after construction, attesting to their durability (Cedergren, 1987). In the early 1800's, John McAdam (1820) stated that if water is allowed to pass through the road into the subgrade, loss of support will occur regardless of the pavement thickness. McAdam also linked poor road performance in Great Britain in the 1800's to ignorance towards the necessity of adequate pavement drainage.

The advent of automobiles and trucks in the early 1900's necessitated the construction of all-weather surfaced roads. Engineers assumed that they could easily design pavements to withstand the large pore water pressures created by free water under the higher load levels. Needless to say, many of these pavements failed prematurely due to water associated distresses. Although the Highway Research Board (HRB) recognized that free water created distress, they did not alter road designs to account for it. In the 1950's, the HRB performed numerous road tests (HRB, 1952; HRB, 1955; HRB, 1962) to determine the effects of axle loads on pavement distress and performance. Not surprisingly, it was found that the largest amount of damage to the pavement occurred when the underlying structure was in a saturated state. Unfortunately, even though these observations were made, drainage systems were not used as a fundamental design feature until the mid to late 1980's (ERES, 1996).

Up until the mid 1980's, it was common practice in the United States to use a dense-graded granular base material. Although this material could be compacted to a high density, the high amount of fine material passing the 75 mm (No.200) sieve resulted in poor drainage characteristics. One example of this type of specification is that formerly used by the Corps of Engineers (COE). Their concrete pavement design criteria required the use of a dense-graded granular base that drained to 50 percent saturation within 10 days (Army, 1965). It was found that their gradation and drainage requirements were in direct conflict as the standard base was effectively impermeable if the gradation was met. This was confirmed by a COE study which found that the subsurface pavement layers of most pavements designed using this criteria remained near or in a saturated condition throughout their service lives (Nettles & Calhoun, 1967).

0.075mm

Former Secretary of Transportation Federico Pena reported that the cost of repairing all backlog highway deficiencies existing at the end of 1991 would be \$212 billion dollars, which was \$7 billion more than in 1989. It is believed by some that the primary reason for many premature pavement failures are distresses associated with saturated subsurface pavement layers (Grogan, 1994). According to Cedergren (1994), "it is the undrainage philosophy pervading the pavement-design profession that is responsible for the premature failure of thousands of miles of pavements." Thus, it has been argued that good drainage design practices could have averted much of the premature damage incurred, saving billions of dollars in highway repair.

In 1973, Harry R. Cedergren, along with Ken O'Brien and Associates, completed the Federal Highway Administration (FHWA) report titled *Guidelines for the Design of Subsurface Drainage Systems for Highway Structural Sections*. This report concluded that the primary cause of distress in numerous cored pavement sections is the abundance of free water within the pavement structure. It put forward the need to drain free water from the pavement structure as a precursor to improved pavement performance. This seminal work became the foundation for a major shift in pavement design practice in the early to mid 1980's, with Cedergren spearheading the revolution.

Recent reports by Forsyth (1993) and ERES (1996) indicate that most States have adopted subsurface drainage procedures. At the time of his report, Forsyth found that 33 States were using drainage systems with their PCC pavements. In the more recent report, ERES obtained survey results from 37 highway agencies, 31 of which were using drainable bases. This major shift occurred over a relatively short time span and with little long-term performance data demonstrating the effectiveness of drainable pavement systems. Only recently have results of studies of in-service pavements constructed on drainable bases become available, although in many cases, the pavements under study have been in service less than 10 years.

3.2 Components of Drainable Pavement Systems

Drainable pavements are designed to provide rapid, efficient removal of water from the pavement structure. A number of informative references are available providing both a justification for the use of positive drainage for PCC pavements and information regarding the design of drainable systems. Some of the most helpful references are: *Drainable Pavement Systems* (FHWA, 1992), *Technical Guide Paper on Subsurface Pavement Drainage* (FHWA, 1990), *Development of Guidelines for the Design of Subsurface Drainage System for Highway Pavement Structural Sections* (Cedergren et al., 1973), *Highway Subsurface Design* (Moulton, 1980), *Pavement Subsurface Drainage Systems* (Ridgeway, 1982), and *Subgrades and Subbases for Concrete Pavements*

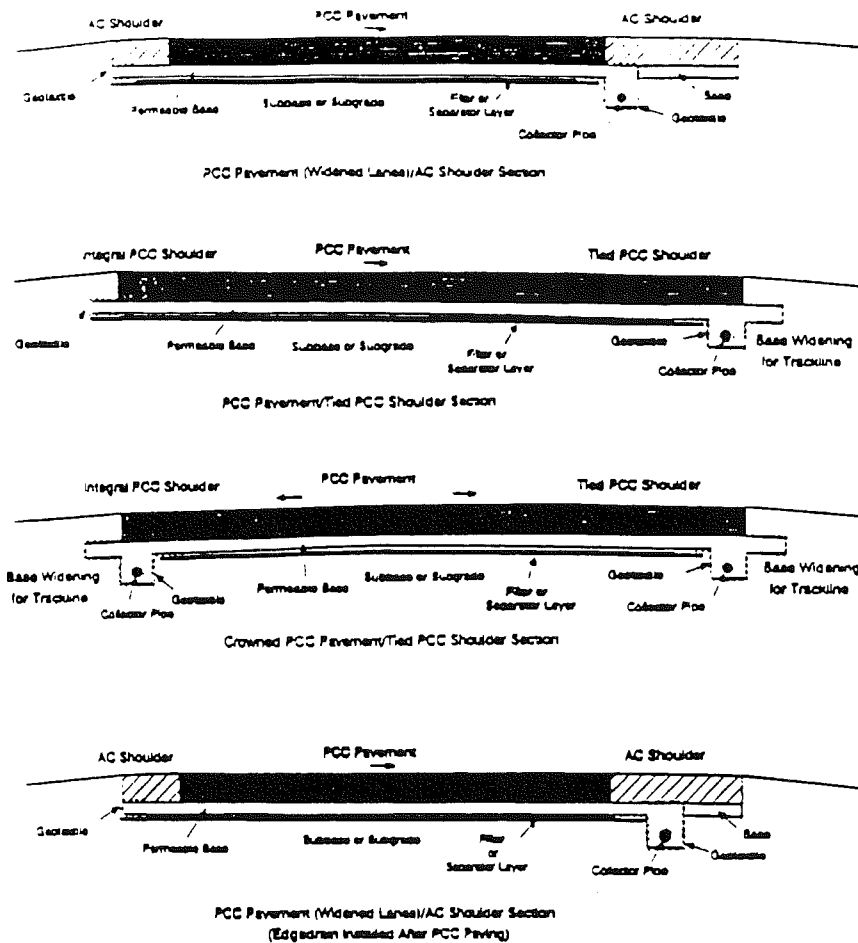
(ACPA, 1995). Additionally, most State highway agencies (SHAs) that are currently using drainable pavement systems have excellent design information (ERES, 1996). Modern pavement drainage systems generally consist of the following primary components:

Permeable Base Layer: A material providing rapid drainage of free water entering into the pavement structure.

Filter/Separator Layer: A material preventing migration of fines (material passing the 75 mm [No. 200] sieve) into the permeable base

Edge Drain Collector System: and adequate transverse outlet pipes to convey accumulated water from the permeable base to ditches or drains.

Geotextile Separators: Geotextiles with designed opening sizes which will prevent migration of fines between layers and into drains but will not clog with fines.



NEED BETTER COPY / INCREASE SIZE

Figure 3.1 Four permeable base sections (FHWA, 1990).

It is critical that the drainage system be viewed holistically, and not as an assemblage of unrelated parts. Too often, the focus is only on the drainable base. It must be remembered that even a well designed, highly permeable, stable drainable base will not function if other elements of the drainage system are improperly designed or constructed. For example, if the filter/separator layer is poorly designed, fine material will infiltrate into the drainage layer, eventually clogging it. If the backfill material is not as permeable as the base, or if a filter fabric is improperly designed or placed, the free flow of water will be hindered and potential failure will result. After all, the drainage system is only as effective as its weakest link and a failure of any one component could result in premature pavement deterioration.

Individual layers of a pavement system must be compatible. For example, if a coarse OGDC material were placed directly on a pure clay sized moist subgrade, eventually we would have a layer of clayey gravel. The drastic difference in particle size makes the two types of material incompatible. The gradations of individual layers can be checked using criteria used established by Cedergren (1962). The general procedure requires that a mechanical sieve analysis be performed on the various layers. The particle size distribution curves are compared and Terzaghi's gradation matching criteria (FHWA, 1994).

The criteria below are recommended to relate the filter/separator layer to the underlying subgrade or subbase material (Moulton, 1980):

$$\frac{D_{15}(\text{filter / separator})}{D_{85}(\text{subgrade})} \leq 5$$

$$\frac{D_{50}(\text{filter / separator})}{D_{50}(\text{subgrade})} \leq 25$$

where D_x is the diameter at which x percent by weight of the particles are finer.

Similarly, these same equations can be used to relate the permeable base and the underlying filter/separator or subbase layer as follows (Moulton, 1980):

$$\frac{D_{15}(\text{base})}{D_{85}(\text{filter / separator})} \leq 5$$

$$\frac{D_{50}(\text{base})}{D_{50}(\text{filter / separator})} \leq 25$$

It is also recommended that maximum percent passing the 75 mm (No. 200) sieve not exceed 12 percent and that the coefficient of uniformity (D_{60}/D_{10}) be greater than 20 and preferably greater than 40, and that minimum layer thickness should be 4 inches (FHWA, 1990).

Geotextile filter/separator layers may also be used in place of the dense-graded aggregate layer, although most States recommend against it. Although the use of a geosynthetic filter may reduce cost of construction, similar design criteria must be met to match the fabric to the subgrade and base. This can be difficult, and it is recommended that the FHWA's *Drainage Pavement Systems Notebook* be consulted when using a geosynthetic filter/separator layer (FHWA, 1992).

3.3 Performance of Jointed Concrete Pavements

Distresses in concrete pavements typically occur in a chain reaction fashion. First, stresses related to fatigue, settlement, and frost heave cause cracks to form in the system. These cracks in addition to contraction and expansion joints then allow water to penetrate the pavement system if not completely sealed. The penetration of water can then initiate many forms of distress on and near these cracks and joints. Pumping action of infiltrated water can cause erosion of fine particles out of the pavement system leaving voids which in turn cause higher deflections and stresses. These higher deflections can result in accelerated spalling and faulting of cracks and joints. Transverse cracks generally deteriorate faster than built in contraction joints due to lack of steel for load transfer effects. Also, the crack faces are more irregular surfaces which are closer together and more susceptible to the effects of trapped incompressible materials. Cracks are generally not sealed, which allows more water in, further accelerating the deterioration process.

3.3.1 The Pavement Environment and Key Mechanisms at Work

To understand pavement behavior it is helpful to think of the following concepts:

Diffusion: Heat and moisture are constantly diffusing through the pavement layers as weather changes from day to night and season to season. The pavement layers act essentially as insulation resting on the earth surface. Because the heat transfer rates and permeability of pavement materials are relatively low, significant gradients of temperature and moisture occur with respect to depth through the pavement system. These gradients cause slabs to curl (temperature) and warp (moisture) causing stress due to non uniform foundation support pressure.

Advection: Fluids can flow also through permeable media due to the presence of a head or potential. For example, the flow rate into a permeable subbase would be faster if 4 inches of water head were resting on the surface of the layer as compared to 2 inches of water resting on the layer.

Stiffness: The relative stiffness of all of the materials controls the structural behavior and stress magnitude for a given set of environmental conditions.

Fatigue: Stress magnitudes along with number of repetitions control “fatigue life” at any given location. A good example of fatigue effects can be seen on M-14 East of Ann Arbor, Mi. The pavements were built in the late 1970’s. After 10 to 15 years of service the driving lane suddenly became rough due to faulting (offsets) of pavement cracks. Stress repetitions exceeding the fatigue life for the concrete crack interfaces occurred in the driving lane resulting in loss of interlock between adjacent panels. A pulse like appearance over time of these types of distress usually occurs associated with materials variations. The passing lane even today has developed very little faulting but is just beginning its fatigue pulse.

Behavior of Rectangular Plate on Subgrade: The geometry of the rectangular plate, for a given thickness and set of environmental conditions, will significantly affect stress levels due to combined gradients and loads. The nature of how it is tied to adjacent plates (dowel and crack opening effects) also significantly affects stress levels during loading of edges and corners, or joints.

Expansion of Freezing Water: Water is a rather unique material in that it expands approximately 9% by volume as it goes through its phase change from a liquid to a solid. This expansion can cause differential pressures on the bottom of concrete slabs resulting in stress.

Water can enter a pavement structure through many different avenues. Figure 3.2 illustrates a number of sources including infiltration through the pavement surface, seepage and lateral moisture transfer, and capillary movement upward from the water table through fine-grained soils (FHWA, 1973). Another source of pavement moisture is vapor movements from groundwater (FHWA, 1990). Many highway engineers believe that subsurface sources of water are the primary contributors to pavement distress, yet it can be shown that infiltrating surface water is also a major source of moisture in the pavement structure (ERES, 1994).

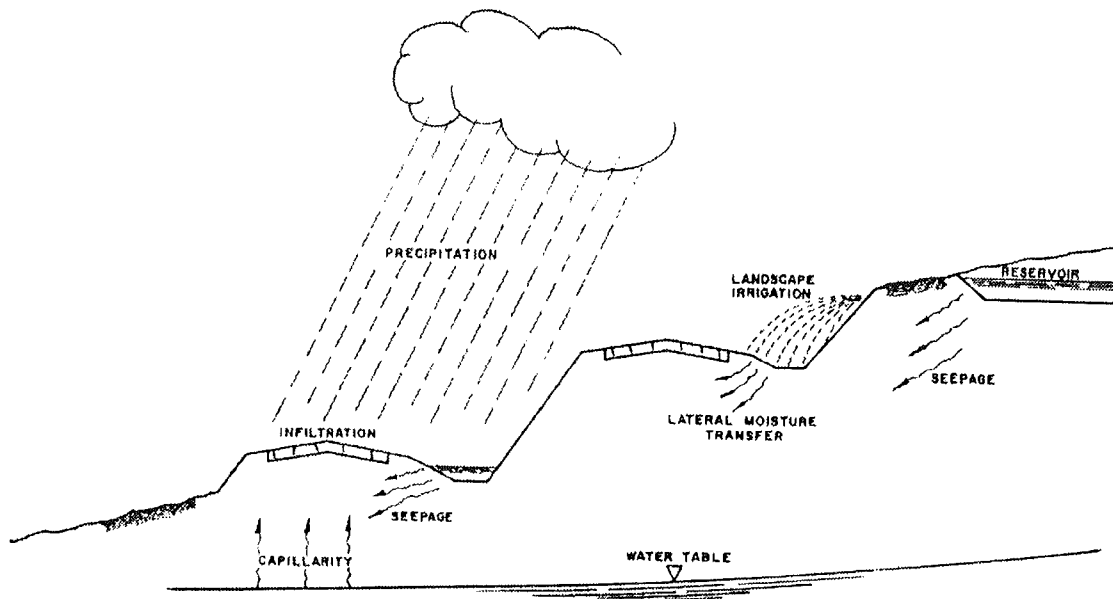


Figure 3.2 Sources of moisture in the pavement structure (FHWA, 1973).

3.3.2 Moisture Related Effects on Distress Development

It is evident that a number of pavement distresses can be directly or indirectly attributed to the presence of moisture in the pavement structure. Pumping, faulting, void formation, and corner breaks are structural defects in concrete pavements that can be directly linked to the presence of free-water beneath the slab (FHWA, 1994). Durability related distresses, such as freeze-thaw damage, D-cracking, and ASR also require moisture. In fact, it is beyond question that the presence of free water in the pavement system is detrimental to pavement performance, leading to a wide variety of pavement distresses (FHWA, 1994).

Once the untreated underlying pavement layers exceed 85 percent saturation, they become highly unstable and vulnerable to the effects of dynamic loading. This includes a significant decrease in strength and stiffness, with increasing susceptibility to non-recoverable strain (Dempsey et al., 1982). At saturated conditions, the effective weight of the soil is reduced, thereby decreasing the effective frictional strength within the soil structure. In his book *Drainage of Highway and Airfield Pavements*, Cedergren (1987) describes in great detail the direct relationship between excess water and decreased pavement life. Some of the adverse effects are manifested in premature rutting, cracking, faulting, increased roughness, and the relative decrease in the level of serviceability (Baldwin, 1987; FHWA, 1994).

When the AASHO Road Test was conducted in 1958-1960, one of the major distresses reported in the PCC pavement sections was pumping. Pumping results when free water present within the pavement structure is ejected from beneath the slab under the action of moving wheel loads. This forceful ejection of water commonly causes erosion, resulting in void formation beneath the corner of the leave slab and subsequent deposition of material under the approach slab. Ultimately, joint faulting results as the approach slab rises due to the build up of material beneath it. This mechanism is illustrated in Figure 3.3.

It is known that faulting is significantly reduced when free water is eliminated from beneath the slab. This is reflected in the AASHTO design guide, which addresses drainage condition through two factors: a loss of support factor (LS) and drainage coefficient (C_d) (AASHTO, 1993). The LS factor is used to modify the effective k-value, reducing it if erodible, untreated granular base is used. The C_d is based on quality of drainage and the percent of time that the pavement structure is exposed to moisture levels approaching

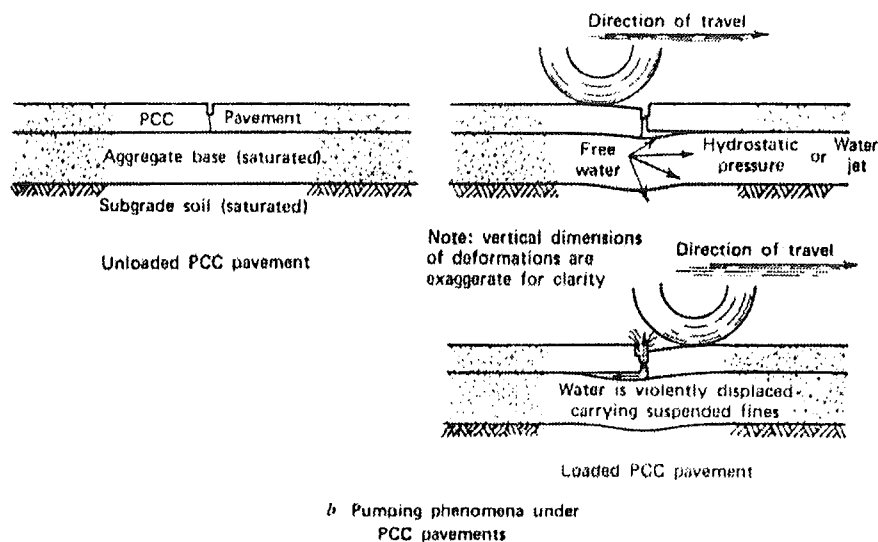


Figure 3.3 Mechanism of pumping which affects faulting and spalling (FHWA 1973b).

saturation. In situations where erodible, non-draining base is used in a location where high levels of saturation are expected, the AASHTO design procedure requires that a thicker slab be used. This is contrary to early findings of engineers such as McAdam who warned that increased pavement thickness is not a substitute for good drainage. Many researchers have investigated the mechanisms leading to pumping and what design elements can be used to mitigate it (Gulden, 1974; Ray & Christory, 1989; Van Wijk et

al., 1989). In high traffic areas subjected to wet environmental conditions, it has been concluded that the most effective method to alleviate pumping is through the installation of a drainage system that rapidly removes free water from beneath the slab.

Others have proposed that the use of drainable pavement systems will reduce material-related distress (MRD) because initiation and progression is dependent on the PCC being at or near saturation. The need for high saturation is true of both physical deterioration, such as D-cracking or paste freeze-thaw damage, and chemical deterioration, such as alkali-silica reactivity (ASR). This trend has been observed in some pavement performance studies which noted a decrease in the incidence and severity of D-cracking in pavement sections constructed on drainable bases (Darter & Becker, 1984; Crovetti & Dempsey, 1991). At this time, the relationship between pavement system drainability and the initiation and progression of MRD is uncertain and further study is recommended (Bunke, 1990; ERES, 1996; Moss et al., 1997).

As a result of the potential improvement in pavement performance, many States have modified their specifications away from dense-graded, poorly draining base material to those featuring more open-graded, drainable base materials.

3.3.3 Apparent Effects of Base Type and Drainage Systems on Pavement Performance

Assessing the performance of drainable bases is not a trivial task. One of the major problems is in how performance is defined. One definition of performance focuses exclusively on how well a drainage system drains free water from beneath the pavement surface. A broader definition of performance encompasses the impact that a drainable pavement system has on overall pavement performance as evidenced by a reduction in distress and improved ride quality. A third definition of performance goes one step further by considering the cost effectiveness of drainage; i.e. "Is the additional cost associated with constructing a drainable pavement system justified through long-term improvement in pavement performance?"

Although irrefutable evidence does not currently exist, trends presented in the literature seem to indicate that good performance has been met as defined by the first two definitions. This belief was stated by Baldwin (1987) who reported in an early study of pavement drainage system performance that 78% of the states using drainage systems report excellent or good performance. But recently, some issues have been raised concerning the cost-effectiveness of drainable pavement systems, but a definitive study on the cost effectiveness of drainable bases has not yet been completed.

Assessing performance as defined by the drainability of the system is not easy because measurement of in-situ moisture contents generally require the use of in-place instrumentation or destructive testing. In either case, the testing is expensive and may be disruptive to traffic. This means that only a few sites can be monitored, thus the data collected may not be representative of the performance of the system as a whole. Difficulties in assessing pavement performance on drainable systems stems from the fact these sections have only been in existence for a relatively short period of time. It is only within the last decade that the use of drainable pavement systems have gained widespread acceptance, and thus there is little long-term information available regarding the effectiveness of drainable pavement systems in reducing pavement distress as compared with pavements constructed on dense-graded bases. As a result, little information related to long-term cost effectiveness is available. The following provides information obtained from published literature regarding the latter two definitions presented above.

A number of studies have focused on the positive impact that improved pavement drainage would have on pavement performance. Cedergren (1987) presented the argument in great detail in his text *Drainage of Highway and Airfield Pavements*. Others have supported this argument with equal enthusiasm, citing the well-documented relationship between the presence of free water beneath the PCC slab and accelerated deterioration. The following discussion presents results of studies examining the relationship between pavement drainage and pavement performance.

Cedergren (1987) presents five case studies describing improved pavement performance resulting from the use of drainable pavement systems. In all cases, he reports a significant reduction in pavement distress as a result of improved pavement drainage. In a more recent article, Cedergren (1994) reports additional case studies in which pavements constructed on drainable systems were performing in an exceptional manner. Many of his citations are anecdotal, and are not part of an organized study in which drainable and non-drainable systems are directly compared.

Illinois has recently detailed some problems with the performance of continuously reinforced concrete pavements (CRCP) constructed on open graded cement treated bases (Heckel, 1997). Premature distress including deteriorated transverse cracks, punchouts, and patching have called into question the applicability of drainable bases for use with CRCP. An investigation into the problem has included visual inspections of the pavement and drainage structures, coring, shelly tube sampling, and FWD deflection testing. Although the underdrains appeared to be in good condition, it was noted that in many cases "the soil at the base of the outlet is higher than the flowline of the outlet." This suggests that during rainfall events, the outlets are likely underwater and water is

backing up into the drainage system. An internal investigation of the drainage system was not conducted nor was in-situ drainability assessed. It was also noted that in two of the three projects suffering premature distress, no filter/separator layer was used “due to the added cost.” Further, it was stated that a significant amount of subgrade infiltration into the drainage layer had occurred. Although the report does not draw absolute conclusions as to why failure occurred, it speculates that one of the following might be responsible:

- the CRCP is incompatible with drainage layers,
- the lack of a filter/separator layer,
- the cement content in the cement treated drainage layer was insufficient,
- the steel was improperly designed or constructed, or
- the design of the CRCP and/or shoulders was inadequate.

This study has direct relevance to the current MDOT study and should be followed closely, as more information becomes available.

Hagen and Cochran (1996) studied various drainage systems and their effect on pavement performance on a reconstruction of I-94. Comparisons were done between an asphalt treated base (permeability of 305 to 610 m/day [1000 to 2000 ft/day]) with a dense graded base (Mn/DOT class 5) both with edge drains. This study found that the least amount of early distress occurred on the permeable asphalt-stabilized base sections. They report that after only six years, jointed reinforced concrete pavement (JRCP) constructed on dense graded bases had five times the mid-panel cracks than that constructed on asphalt treated permeable base. Also cited was another study conducted on TH 15 in southern Minnesota. This section of pavement was constructed in 1983 and examined in 1994. Negligible mid-panel cracking was observed in the pavement sections constructed on asphalt treated permeable base compared to 95 percent cracking of slabs on the section constructed on dense graded base. It was noted that the drainage systems were well maintained and properly constructed and were draining as desired. Overall, this study recommends that “all concrete pavements need some type of positive subsurface drainage system.”

Crovetti (1991) cites five recent cases in which States monitoring the performance of pavements constructed on open-graded and dense-graded bases universally report that pavement distress was significantly reduced on the open-graded pavement sections (Crovetti, 1991). In California, PCCP constructed on drainable bases have shown consistently lower slab cracking rates than those constructed on dense graded bases. A PCCP test section was constructed in Michigan in 1975 to compare permeable, bituminous, and dense graded bases. It was observed that the pavement constructed on

the permeable base had the least amount of recorded faulting, slab cracking, and D-cracking. Similarly, a Minnesota study conducted in 1983, which compared drainable and non-drainable PCCP sections, found significantly less slab cracking on the drainable sections after five years of service. Croveti also cited studies in New Jersey and Pennsylvania in which drainable PCCP sections had significantly less distress than pavements constructed on dense graded base.

Croveti (1995), frustrated with the limited performance data available due to the relatively short time-frame for which drainable bases have been used, developed non-destructive testing methods to provide insight into design efficiency. These analytical techniques quantify the uniformity of support under a slab utilizing slab dimensions, measured center, edge, and corner slab deflections, and in-situ temperature gradients. Croveti used the results of this analysis to examine the potential performance of pavements constructed with drainable bases on USH 18/151 in the fall of 1994. At the time of testing, the test pavement was five years old. The base types investigated were untreated drainable, cement-treated drainable, asphalt-treated drainable, dense-graded, and lean concrete. The only sections found to have evidence of poor support due to densification or erosion of the base layer was constructed on untreated drainable base, although additional data would need to be collected to confirm this finding (Croveti, 1995; Croveti, 1996). At this time, long-term performance data is needed to verify the applicability of the test method.

California found that the use of subdrainage significantly reduced faulting of jointed plain concrete pavement (JPCP) (Wells, 1985). This study also found that slab cracking was reduced through the use of drainage. Forsyth et al. (1987) showed that in California, slab cracking was 2.4 times greater on undrained pavement sections than on drained pavement sections. More recent examination of data from California (Wells, 1991) have shown that drainage pavement systems are capable of draining large quantities of water, but suggest that long-term pavement performance has not been investigated, noting that there are some concerns in this area.

In an FHWA study, Smith et al (1990) concluded that drained concrete pavement sections appeared to have improved performance over adjacent undrained sections, although no definitive estimates of extended life were provided. This original study was later expanded to include over 300 in-service PCC pavements. In this more recent study, drainage was not found to be a significant factor contributing to slab cracking, but lead to a decrease in D-cracking in some cases (Smith et al., 1995).

In a recent study completed by Northwestern University (Moss, 1997), drainage was found to be a significant factor in the development of premature distress in concrete

pavements. This study focused exclusively on the development of undiagnosed materials-related distress, but a thorough statistical analysis determined that improved drainage through the use of drainable pavement systems resulted in a decrease in the incidence of premature distress.

3.3.4 Other Important Factors Affecting Transverse Cracking of Jointed Concrete Pavements

A significant area of study in jointed concrete pavements is related to identifying the factors affecting transverse cracking in concrete pavements. Curling typically refers to deflections caused by the effects of temperature differences through the thickness of the slab causing deflection of the edges of the slab relative to the center. Cooler temperatures on top of the slab compared to the bottom would result in the corners lifting up relative to the center of the slab due to thermal contraction of the upper portions of the concrete. Gravity then pushes these uplifted corners back down causing tension on the top of the slab. Warping refers to deflections caused by differences in moisture content through the thickness of the slab. Slabs generally have greater moisture loss/desiccation on the upper surface relative to the lower surface resulting in greater shrinkage of the upper surface. This results in the edges of the slab lifting upward relative to the center. Measured temperature and moisture distributions through the slab thickness have been shown to be non linear by many investigators (Teller, 1935, Janssen, 1996, Rhodes, 1949) and can be quite severe when the pavement layers pass through the freezing point. If considerable moisture exists in the base layer, it will remain at the 32 degree F point for quite some time before actually freezing as the required calories are lost during the phase change. At the same time, the ambient air conditions may fall way below freezing causing very large gradients through the slab thickness.

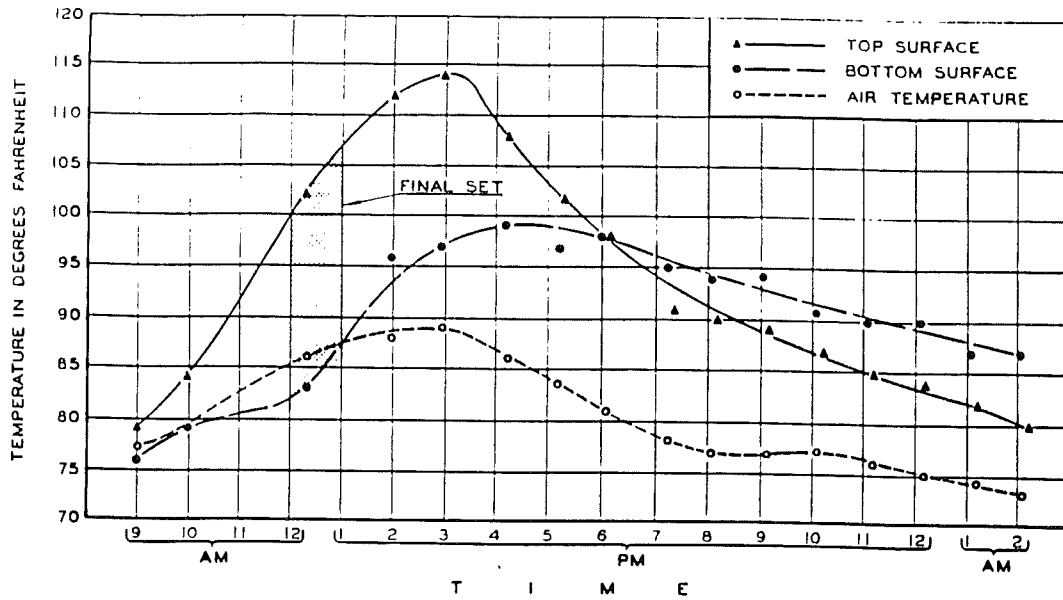
These temperature and moisture effects begin at early ages, often referred to as construction curling, developing immediately after placement of the concrete on grade. During hydration, a thermal gradient, either positive or negative, will develop in the plastic concrete. A typical morning pour would likely develop a significant warm on top type gradient by the time of set. Figure 3.4 shows measured temperature gradients immediately after placement for a relatively warm condition morning pour in Michigan (Rhodes, 1949). After cooling, the edges may lift upward relative to the center, due to this gradient condition which was present at set while the slab was flat and stress relaxation/creep effects, as temperature gradients reduce back toward zero. Moisture loss occurs more rapidly off the top surface relative to the bottom surface. This would be more pronounced for dry, hot weather paving where mix temperatures and curing techniques would be more critical factors in gradient development and evaporation rates. During hot weather paving the resulting heat development is faster causing a higher

overall temperature and temperature gradient at set. At these higher temperatures, faster rates of evaporation would likely exist. It is these resulting high tensile stresses on top of the slab that are likely in part responsible for more top down cracking observed for hot weather pours. We currently lack a thorough understanding of the interactions between these factors, especially for the early ages of the pavement system, with respect to predicting where and when cracking will occur. Warping has been shown to be related to regional relative humidity . Table 3.1 shows the apparent effect of factors causing bending stresses in pavement slabs for top and bottom of slab damage during cool on top (early morning) and warm on top (mid afternoon) temperature conditions.

Table 3.1. Summary of effects of various stress factors which contribute to transverse cracking.

Stress Input	Early Morning(Upward Curl)		Mid Afternoon(Downward Curl)	
	Stress (Top)	Stress (Bottom)	Stress (Top)	Stress (Bottom)
Average Temperature	tension	tension	compression	compression
Temperature Gradient	tension	compression	compression	tension
Subgrade Friction	tension	tension	compression	compression
Construction Curling	tension	compression	tension	compression
Concrete Shrinkage	tension	tension	tension	tension
Moisture Gradient	tension	compression	tension	compression
Joint Loading	tension	compression	tension	compression
Mid Pannel Loading	compression	tension	compression	tension

Theoretical analysis (Westergaard, 1925) indicated that the location of maximum thermal stress for cool on top conditions should be located between $4.3l$ and $5.7l$ where l is the radius of relative stiffness of the pavement system. The magnitude of the stress at this location was predicted to be about 10% larger than the fully restrained thermal stresses in the interior portions of the slab. FEM analyses (Byrum, 1994) also indicated that the maximum stress would be at this location for jointed slabs and that this location was typically the point of maximum stress due to combined thermal and load effects.



TEMPERATURES of PAVEMENT SLAB POURED at 7:30 A.M.

Figure 3.4 Early age temperatures and resulting curling (Rhodes, 1949)

4. EXPERIMENTAL DESIGN

4.1 Selection of Test Sections

Because more than 650 lane miles of concrete pavement in Michigan have been built on Open Graded Drainage Courses (OGDC) since 1980, it would be impossible to study each pavement section in detail. At the same time, this large investment in OGDC systems merits a careful investigation of the influence of these bases on pavement performance. Thus, representative study sections must be chosen that will provide evidence of the influence of the base course on the performance of the entire system. A complete listing of all OGDC pavements in Michigan is found in Appendix A.

While historical records, pavement management system data (PMS) and ride quality index data (RQI) can be used to give some indications of distress development in various pavements, these cannot replace detailed field evaluation and laboratory testing. In a limited duration study, though, where field evaluation of pavements is only possible at one point in time, it is difficult to pin-point the development of distresses. For this reason, it is valuable to choose study sections that represent long-term performance, while also studying performance of other pavements early in their service lives.

Because Michigan has only been using OGDC systems since the early 1980's, "long term performance" in this study refers to pavements that have been in service for at least 10 years.

Long-term performance study

In order to evaluate the longer-term performance of OGDC pavements, six pavements supported by OGDC were selected representing a wide range of distress levels (as characterized by transverse cracking, spalling, and faulting). Three additional sections on Dense Graded Base Courses (DGBC) were chosen for comparative purposes. Initial selections were made by reviewing PMS and RQI data, historical records, and recommendations by MDOT TAG. Of particular interest in the historical records were the gradation specifications of the base course materials. Final selections were made after walk-throughs in the field confirmed the available distress data.

Efforts were made in site selection to minimize the effects of other variables such as traffic volumes, slab length, and pavement age.

The studied sections range from 10 to 16 years in age, with all but 2 being between 10 and 13 years old. All sections but one have 41 ft transverse joint spacing. The remaining section has 44 ft joint spacing. All have 12 foot wide traffic lanes, and 9 inch thick concrete supported on a 4 inch thick base course. All have, concrete shoulders, most of which are subdivided by intermediate shoulder joints. Traffic ranges from 178,900 to 455,300 total lane ESAL's/year in the truck lane. While this does suggest considerable variation in traffic levels, none of these sections represent extremes in traffic volume.

All of the study sections except one were selected along the I-69 corridor between Port Huron and Lansing. The additional section is located on I-475 in Flint, within a few miles of I-69. This close proximity helps to reduce climatic effects such as number of freeze-thaw cycles on the pavements.

The nine chosen sections for the long-term performance study are shown in Table 4.1 below. Detailed site information on each test section is found in Appendix B.

Table 4.1 Pavements selected for the long-term performance study.

Route	CSN-Job#	Location	Job Length	Year Constructed	Base* Type
I-69	19042-02233A	EB, Webster Rd to Upton Rd	3.6	1987	8G
I-69	19042-24680A	EB, Chandler Rd to Webster Rd	2.6	1986	8G
I-69	19043-02234A	EB, Airport Rd to US27	3.1	1981	22A
I-69	19043-02234A	WB, Airport Rd to US27	3.1	1981	22A
I-475	25132-06582A	SB, Steward Rd to Coldwater Rd	2.5	1981	22A
I-69	44044-18804A	WB, M-24 to East of Wilder Rd	3.7	1984	8G
I-69	77023-21586A	EB, M-19 to GT&W RR	10.4	1984	8G
I-69	77024-17988A	EB, Cox-Doty Drain to M-19	5.6	1984	8G
I-69	77024-20821A	EB, Countyline to Cox Doty	5.8	1984	8G

* This is the base as specified at construction. Sieve analysis may show that the base fits a different gradation.

New Construction Study

The study of newly constructed sections includes 3 sections that were 2 years old at testing, and two sites that were under construction at time of testing. The 3 sections that were 2 years old at testing are located on I-94 near Waternvelict. They were selected because premature distress had been observed there, and it was believed that the OGDC might be a contributing factor (in) the distress.

FOR

The two sections under construction at the time of testing were similar in design to the three sections on I-94, and allowed for instrumentation of the slabs and observation of the construction process.

Table 4.2 shows the 5 sections studied in the new construction study.

Table 4.2 Pavement sections selected for the new construction study.

Route	CSN-Job#	Location	Job Length	Year Constructed	Base Type
I-94	11017-32516A Sec A	EB, East of Park Rd	2.0	1995	3G
I-94	11017-32516A Sec C	EB, West of Carmody Rd	1.5	1995	3G
I-94	11017-32516A Sec D	WB opposite sections A-C	5.0	1996	3G
I-96	47065-28215A	EB & WB, East of D19 and West of Dorr Rd	3.6	1997	3G
I-275	82291-37305A	NB, Central RR to Wabash Rd	9.4	1997	350AA

4.1.1 PMS

In order to assist in the selection of test sites, pavement management system (PMS) data was used. PMS provides a distress index for every tenth of a mile of pavement. The distress index is a number that ranges from 0 to 100 (0 representing a perfect pavement) and is used to quantify the amount of distress that is present. PMS takes into account transverse and longitudinal cracking, damage at joints and any mud jacked slabs or shattered slabs that might be present. All of this distress is then quantified and used to obtain the distress index.

In this study PMS was used to look at potential test sections and specific test sites within candidate sections. The PMS data ^{was} reviewed to locate sections of low, medium and high distress. PMS data also provided an understanding of the types of distress present. Finally PMS data gave a measure of the variability within test sections. As an example Figure 4.1 shows the 1995 PMS data for control section 77024 eastbound. The two test sites chosen from this control section were at milepost 1.3 to 1.4 and 7.5 to 7.6. It can be quickly seen in the figure that significant differences in performance can be expected. Furthermore, it can be noted from the figure that a sudden drop in distress index occurs near milepost 5.8. This location represents the border between two separate

NO PMS limit
 NO, JUST A PAVEMENT w/ distress
 examples - not inclusive

paving contracts. Review of the PMS data ^{have} has shown that it is not uncommon to see specific distress signatures associated with individual paving contracts. X

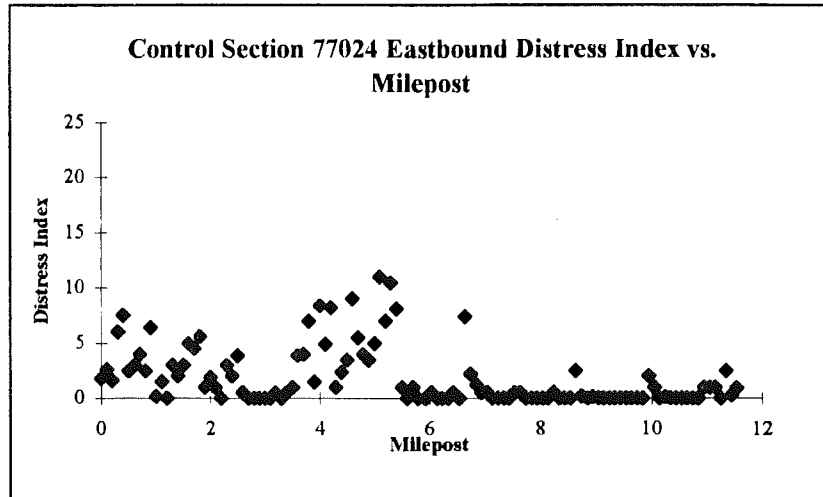


Figure 4.1 The PMS data for control section 77024 EB.

The 1995 PMS data for the control sections studied is found in Appendix F of this report.

4.1.2 RQI

To help in the selection of possible test sites, Ride Quality Index (RQI) data was also reviewed. RQI is a measurement of a pavement's surface profile. This information is obtained by using a profilometer driven down the (two) wheel paths of a lane. This change in surface profile is then quantified as RQI. The RQI is averaged over every tenth of a mile. RT only

By having RQI data from 1992 through 1995 available, the research team was able to review the rate of change of the surface profile over time. RQI was the only available measure of deterioration rate, and was thus a valuable tool in selecting a site. As an example two pavements with similar RQI values can be distinguished by their deterioration rates. One would be much more concerned over a pavement that is WERS

Need to better describe what RQI is

deteriorating rapidly, then one that developed some roughness early in its life but has been stable since.

In the figures below one can see the RQI data and the RQI growth rate for control section 77024 EB. Figure 4.2 shows the RQI data for 1992-1995. The milepost tested on this control section were 1.3 to 1.4 and 7.5 to 7.6. This figure shows that these two locations have very similar RQI values.

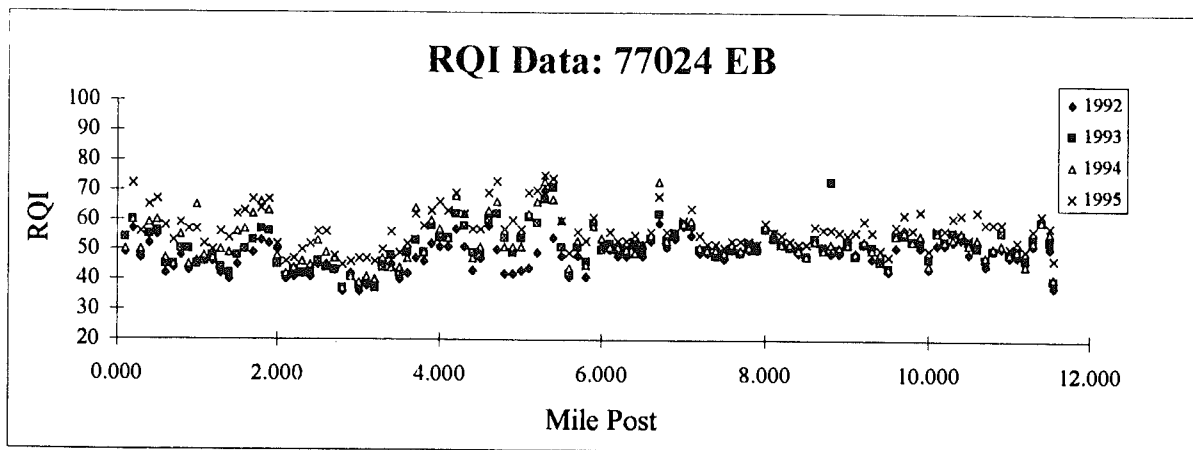


Figure 4.2 RQI data for Control Section 77024 EB

In Figure 4.3 below, the growth rate of the RQI data ^{ARE} (is) shown. ^{that} This figure again shows clearly the border between the two paving contracts at milepost 5.8 ~~which~~ ^{which} agrees with PMS Data.

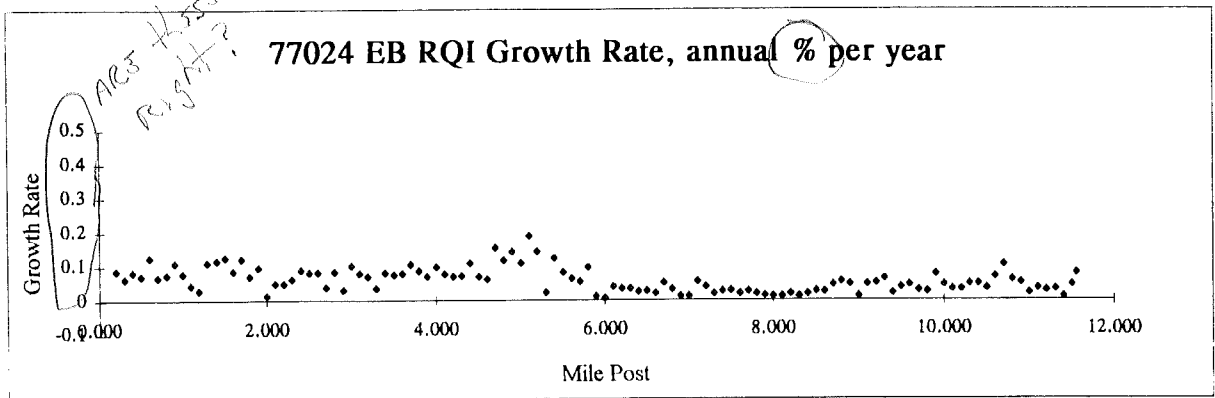


Figure 4.3 RQI Growth Rate of the RQI data for Control Section 77024 EB

RQI data for each of the selected control sections is found in Appendix F.

4.1.3 Historical Records

Through the use of historical records additional information about potential test sites was obtained. The historical records contain the mix designs used, base and subbase gradations, weather during construction, and inspector's daily reports that give detailed information about construction. The historical records complement the information obtained from PMS and RQI, and can highlight potential causes of distress development.

4.1.4 Field Condition Survey

After a review of the PMS data, RQI data and historical records, a field condition survey was performed to finalize site selection. This survey was a walk through of a potential site to verify information obtained in PMS, RQI and the historical records. The types of distress present and ^{SP}(there) severity are investigated further during the on site survey. Additionally, the drainage of the site and the traffic volume present at this time are

observed. After field condition survey, final descisions can made as to the suitability of a given test location.

4.2 Field Testing Procedures

In order to quantitatively and qualitatively evaluate the performance and condition of a selected test site, both field and laboratory testing programs were conducted. The data gained from these investigations, combined with the PMS, RQI and historical records were used to compare and contrast the various pavement systems.

Within each selected pavement section, a 500 ft (1000 ft in some cases) long test section was chosen that was representative of typical distresses found on the site. Where possible, special features such as inclines, culverts, overpasses, sharp turns, and ramps were avoided. Testing typically began early in the morning and continued throughout the day.

Once ^{the} 500 ft test section had been selected based on a preliminary walk-through of the site, lane closure was established. The pavement was then marked to indicate locations for core samples and FWD measurements. Once the FWD and coring crews had been mobilized, a thorough distress survey of the site could be performed, along with a drainage survey and photographic record. Distress surveys included locations of cracks, spalls, core locations, FWD locations and other minor distress. As well as measurement of crack widths and slab faulting.

Falling weight deflectometer testing started as soon as lane closure was available and the site had been marked. FWD testing was repeated in the afternoon. On some sites, when weather conditions were changing rapidly, FWD testing was performed 3 times during the day.

As soon as the FWD crew had proceeded past the first coring location, the drilling team began taking concrete core samples. Core drilling was followed by DCP measurements and soil sampling.

In the subsections that follow, each of the field testing methods and procedures are discussed in detail.

4.2.1 Site Photos

Photos of each test section were taken to create a visual record of each site at the time of testing. The photographic record includes overview photos showing the contour of the land and the general layout of the site. In addition, photos of each tested slab were taken. These photos show locations of distresses, coring and FWD locations, and transverse joints. Special features of the sites were also recorded, such as close-up views of drainage structures, coreholes, and distresses.

In Appendix D of this report, a few representative photos from each site have been included to give the reader a quick overview of the various test sections.

4.2.2 Distress and Drainage Surveys and Crack Width Measurement

Distress surveys for each test site were conducted showing in detail the locations of coreholes, FWD tests, transverse joints, transverse and longitudinal cracks, spalling, faulting, and other surface distresses and notable features. Cracks were measured for width and length. A crack comparator card was used to measure average crack widths to the nearest 0.1 mm. Crack lengths were recorded if the crack did not span the entire lane. Faulting was measured to the nearest 0.1mm. using a faultmeter. Other features noted include sewer grates, delaminations due to high steel, and significant pop-outs. A portion of a typical distress survey can be seen in Figure 4.4.

Drainage surveys were conducted to detect any potential water-related problems in the pavement systems. Notations included locations and conditions of edge-drain outlets, clogging of drain outlets, standing water in the ditches, growth of swamp vegetation in ditches, condition of drainage structures in the median and other notable features.

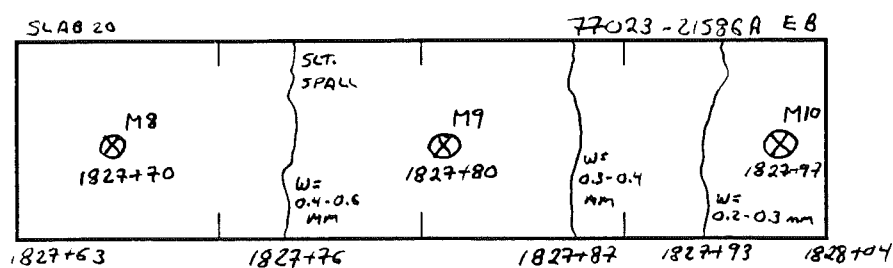


Figure 4.4 A typical Distress Survey.

The distress surveys are found in Appendix C of this report.

4.2.3 Concrete Coring

Concrete coring was conducted in accordance with ASTM procedure C 42-94 (by MDOT personnel). The cores were labeled with an identifying number and station location. Concrete was cored for laboratory determination of compressive and split tensile strength, elastic modulus, and pavement thickness determination. In addition, the coring locations provided access to the underlying foundation. A minimum of six cores were taken from undamaged areas in the middle of slab panels. Three of these cores were used for compressive strength and elastic modulus determination, and the other three for split tensile strength. Additional cores were taken from cracks and transverse joints to evaluate dowel bar condition, to make qualitative observations of the crack surfaces.

4.2.4 DCP Testing

Dynamic cone penetrometer testing was performed using the U.S. Army Corps of Engineers DCP apparatus. DCP tests were performed at 5 to 6 locations on each site at the mid-slab coreholes. DCP values were recorded as millimeters of travel by the DCP shaft versus blowcount on the anvil. One blow refers to dropping a 10.1 lb. weight onto an anvil from a standard height of 22.6 in.

Correlations are found in the literature to relate mm/blow for DCP to California Bearing Ratio (CBR). The correlation recommended by the U.S. Army Corps of Engineers is:

$$\text{CBR}(\%) = 292/\text{DCP}^{1.12} \quad \text{[Eq.4.1]}$$

Is this RIGHT?

The correlated CBR values have been calculated for this project's data in Appendix I. It should be noted, though, that the correlations may not be well suited for the soil types encountered in this study. Thus, the CBR correlations should be considered only provisional.

The value of DCP measurements is that they provide a direct measure by which to compare the stiffnesses of different coreholes and test sites on a relative basis. Figure 4.5 shows the variation of average base and subbase DCP values over a 500 foot test section.

Base values reported here are mm/blow values averaged over a depth of 0 to 75 millimeters below the concrete. Subbase values are averaged from 150 to 250 millimeters below the concrete. Variations over the job length are qualitatively representative in differences in foundations stiffness. It should be noted that the lower DCP values for the base course are likely caused by a loss of confinement after coring.

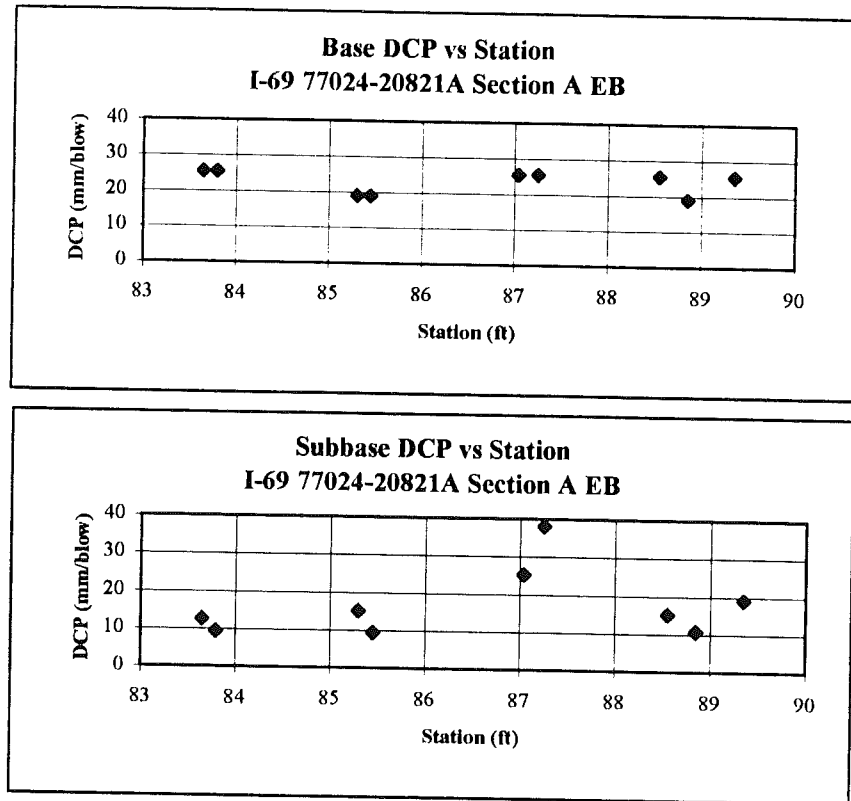


Figure 4.5 DCP vs Station

4.2.5 Soil Sampling

Soil samples were taken from the base, subbase, and subgrade of each mid-panel core location for each test section using a handheld soil auger. Where embankment material was present, it too was sampled. On some sections subgrade samples could not be obtained. The samples labelled and taken to the laboratory for loss on wash and

by



gradation analyses. Based on the resulting gradation curves filter criteria and foundation permeability were calculated.

During soil sampling, the depths of the various foundation layers were recorded. The pavement system profiles found in Appendix B result from these records. The distinction between subbase and subgrade was sometimes unclear, and the depth of the transition was estimated on many sites.

4.2.6 FWD Testing

This section will be included and explanation of FWD testing in the final report.

4.3 Laboratory Testing

Once soil samples and concrete cores were obtained from the selected test sections, they were taken to the laboratory for testing. The lengths of six cores were measured before cutting with a diamond blade to establish two flat surfaces. The smallest possible amount was cut to maintain the longest specimen. Three of the cores were then capped according to ASTM C 617-94, with sulfur capping compound to insure plane and level surfaces at both ends. The capped length of the cores were then measured. The specimens were then ready for testing. The other three cut cores were then measured in preparation for split tensile testing.

Soil samples were placed in zip-loc bags and sealed. Upon returning to the laboratory, the soil samples were oven dried. Once dry, the soil sample were ready for loss on wash testing and gradation testing.

4.3.1 Concrete Properties

Three of the capped specimens are then tested in compression according to ASTM C 39-94. The elastic modulus was determined according to ASTM C 469-94. The remaining three cores were tested for split tensile strength according to ASTM C 496-90.

Appendix G shows the concrete properties for all sections tested.

4.3.2 Gradation - Loss on Wash and Sieve Analysis

Loss on wash was performed on the dense graded base course samples, as well as subbase and subgrade samples from all sections. This test was performed according to ASTM C 117-95. Sieve analysis was performed in accordance with ASTM C 136-95. After much of the sieving was completed, it was observed that ASTM limits on amount of material retained on a sieve had been exceeded for a number of samples. The potential impact of this error was of concern to the research team. For this reason, sieve analysis was repeated for about 20 samples where the limits had been exceeded. The results from this sieving were then compared to the original sieving results. It was found that there was no significant impact from exceeding sieve weight limits. This gave the research team the needed confidence to continue analysis with the existing data.

4.3.3 Filter Criteria, Hazen Permeability

After loss on wash and sieving were performed on the soil samples filter criteria developed Moulton was applied. The criteria that was used and its results are shown in appendix H.

4.4 Resilient Modulus Laboratory Procedure

The LTPP Protocol P46 Resilient Modulus of Unbound Granular Base/Subbase Materials and Subgrade Soils (1996) was followed as closely as possible throughout this portion of the laboratory investigation. This procedure is based on AASHTO T292-91I *Resilient Modulus of Subgrade Soils and Untreated Base/Subbase Materials*. Sample preparation was done according to the specifications within the P46 protocol. A split mold was constructed to house the 152-mm (6") diameter by 304-mm (12") high samples. The following outlines the experimental setup and laboratory techniques used.

Two types of aggregate were used in this study: a glacially derived material and a quarried limestone. Each aggregate type was sieved into the following size fractions: 25.4, 12.7, 4.75, 2.36, 0.6, 0.075 mm and pan. The aggregate was then recombined into samples according to the appropriate MDOT gradation presented in Table 4.3.

Why not use gradations found at sites?

why?

Table 4.3 Percent retained by weight for the MDOT 21AA, 350AA, and 3G gradations.

	Percent Retained by Weight							
Sieve, mm, mm	25.4	12.7	4.75	2.36	0.6	0.075	pan	Total
21AA								
Percent retained	7.50	30.00	20.00	10.00	15.00	12.50	5.00	
mass (g)	988.81	3955.25	2636.8	1318.4	1977.6	1648.0	659.2	13184.1
mass (lbs.)	2.18	8.71	5.81	2.90	4.36	3.63	1.45	29.04
350 AA								
Percent retained	5.00	40.00	22.50	10.00	12.50	7.50	2.500	
mass(g)	659.21	5273.66	2966.4	1318.4	1648	988.81	329.6	13184.1
mass (lbs.)	1.45	11.62	6.53	2.90	3.63	2.18	0.726	29.04
3G								
Percent retained	5.00	40.00	27.50	12.50	7.50	7.50	0.00	
mass(g)	659.21	5273.66	3625.6	1648.0	988.81	988.81	0.00	13184.1
mass (lbs.)	1.45	11.62	7.99	3.63	2.18	2.18	0.00	29.04

Three samples were made for each gradation with each material type. This produced a total of 18 samples that were tested in the following moisture states: dry, drained and undrained. The dry condition is defined as the 2-3% moisture content present in the aggregate immediately following sample compaction. This moisture condition is representative of a newly placed base course in the field subjected to minimal traffic and no exposure to moisture.

The second moisture condition investigated was the drained condition. After completing testing in the dry condition, the drained condition was achieved by completely saturating the sample from the bottom up for 12 hours and then allowing it to drain for two hours prior to testing. This moisture condition was designed to simulate a base course connected to a working drainage structure that allows water to freely flow through

gravitational forces alone. A drainage period of two hours is the recommended drainage time for open graded material as defined by Cedergren and the FHWA.

Once testing was completed in the drained condition, the sample was again completely saturated, but this time all the drains were closed during testing. A specimen tested under this situation is referred to as being in an undrained moisture condition. This testing was designed to represent a base course without drainage or one connected to a clogged drainage system in the field. Testing under these conditions significantly reduces the resiliency of the aggregate base course. Pore water pressure was monitored throughout the testing sequence to obtain B parameter results (Note: the B parameter = u/σ_3 where u is the pore water pressure and σ_3 is the confining stress). When the pore pressure was equal to the cell pressure the B parameter is equal to unity therefore indicating a saturated state exists.

Compaction was accomplished using an electric Makita demolition hammer. The hammer weighed 9.4 kg (20.7 lbs.) and was capable of 2000 blows per minute. The material was compacted in six, 50-mm (2 in) lifts to achieve a total sample height of 305-mm (12 in). A 0.55mm (0.022 in) rubber membrane was placed between the mold and granular material to help support the sample throughout the testing sequence. The amount of time required to compact each lift varied according to the material type and required density. The optimum densities were obtained from MDOT and verified by MTU using the modified proctor test method. Table 4.4 summarizes the densities typical of the aggregate and gradations used in this study.

Table 4.4 *Typical modified proctor densities.*

Material Type	Gradation	Optimum Density (Mg/m ³)	95 percent of Optimum (Mg/m ³)
Quarried Limestone	21 AA	2.26	2.14
	350 AA	2.08	1.98
	3G	2.05	1.95
Glacially Derived	21 AA	2.30	2.19
	350 AA	2.13	2.02
	3G	2.10	1.98

Testing was accomplished with a closed loop servo-hydraulic MTS testing system. MTS technicians and MTU researchers calibrated the system prior to testing. The MTS system had a 24.5 kN (5.5 kip) load cell and a 98 kN (22 kip) frame. Table 4.5 presents the testing sequence established in the P46 protocol, including the confining pressure, maximum axial stress, cyclic stress, contact stress, and number of load applications for each step. Each specimen in each moisture condition was subjected to this sequence.

Table 4.5 *Testing sequence for base/subbase materials.*

Step Number	Confining Pressure		Maximum Axial Stress		Cyclic Stress		Contact Stress		No. of Load Applications
	kPa	psi	kPa	psi	KPa	psi	kPa	Psi	
0	103.4	15	103.4	15	93.1	13.5	10.3	1.5	500
1	20.7	3	20.7	3	18.6	2.7	2.1	0.3	100
2	20.7	3	41.4	6	37.3	5.4	4.1	0.6	100
3	20.7	3	62.1	9	55.9	8.1	6.2	0.9	100
4	34.5	5	34.5	5	31.0	4.5	3.5	0.5	100
5	34.5	5	68.9	10	62.0	9.0	6.9	1.0	100
6	34.5	5	103.4	15	93.1	13.5	10.3	1.5	100
7	68.9	10	68.9	10	62.0	9.0	6.9	1.0	100
8	68.9	10	137.9	20	124.1	18.0	13.8	2.0	100
9	68.9	10	206.8	30	186.1	27.0	20.7	3.0	100
10	103.4	15	68.9	10	62.0	9.0	6.9	1.0	100
11	103.4	15	103.4	15	93.1	13.5	10.3	1.5	100
12	103.4	15	206.8	30	186.1	27.0	20.7	3.0	100
13	137.9	20	103.4	15	93.1	13.5	10.3	1.5	100
14	137.9	20	137.9	20	124.1	18.0	13.8	2.0	100
15	137.9	20	275.8	40	248.2	36.0	27.6	4.0	100

The testing software records all the relevant information for each load pulse including both the input stress levels and the resulting resilient and permanent vertical strain. Using this data, the resilient modulus of the material can be computed for each load application and the accumulated permanent deformation can plotted. testing software records all the relevant information for each load pulse including both the input stress levels and the resulting resilient and permanent vertical strain. Using this data, the resilient modulus of the material can be computed for each load application and the accumulated permanent deformation can plotted.



5. STUDY OF RESILIENT MODULUS AND AASHTO SERVICEABILITY FOR OGDC PAVEMENT SYSTEMS

5.1 Resilient Modulus Study on Two OGDC Materials and One DGBC Material

As mentioned earlier in Chapter 4, this part of the study evaluated two different aggregate materials: a glacially derived processed aggregate and a quarried limestone. The glacially derived materials were incorporated into a glacial ice mass from a variety of locations resulting in a wide range of material types. As the glacier moved, the incorporated materials underwent dynamic crushing which completely destroyed weaker particles while rounding the stronger material. Consequently, only strong, highly resistant rocks survived, resulting in a quality aggregate source as the more weatherable minerals were eliminated. But the glacial grinding processes produced semi-rounded or subangular particles that inherently possess poor interlock characteristics. Thus some artificial crushing was required to induce fractured faces to enhance the material's mechanical properties. The material provided to MTU had undergone partial crushing, with most particles having one to two fractured faces. This significantly improved the mechanical behavior of the aggregate compared to a completely rounded aggregate source.

The second type of aggregate studied was quarried limestone. This material was blasted and crushed at a quarry, resulting in a 100 percent crushed material. The mechanical properties of materials produced in this manner will be highly dependent on the quality and variability of the parent rock. The aggregate sent to MTU for this study was coated with fines and had cemented together in the canvas bags during shipping. As a result, it was necessary to sieve the material for extended periods of time to remove the excess fines from the coarse aggregate particles.

As described in Chapter 4, each aggregate type was sieved into the various size fractions and then recombined into the gradations presented in Table 4.3. Compaction was accomplished using an electric Makita demolition hammer. Since the hammer generates a constant force, the time required to densify a given specimen varied depending on the difficulty to achieve compaction. The 21AA gradations were the most difficult to compact in the laboratory, requiring the most input energy and time. The 350AA and 3G samples all were compacted to 98 percent density or greater whereas the 21AA samples were in the 95 to 96 percent range (See Appendix C for complete details).

Note that laboratory compaction is done within the confines of a rigid mold and thus does not accurately reflect potential difficulties in achieving density under field conditions.

The resilient modulus (M_R) values were calculated from the results of the testing by dividing the applied deviator stress (σ_d) by the resultant resilient strain (ϵ_r). The magnitude of applied deviator stresses used in each step is summarized in Table 4.5. The resilient strain is calculated, being equal to the recoverable deformation divided by the specimen height. Table 5.1 summarizes the mean and standard deviation values of M_R for each material type, gradation, and moisture condition (see Appendix K for detailed data). As is seen in the table, the most resilient gradation for the dry and drained portion of the testing sequence was the 21AA gradation. Both the glacial and quarried dense graded (21AA) gradations displayed consistent resiliency if drainage was provided (Range of M_R 430 to 350 MPa). Although the resilient modulus values for the 350AA and 3G gradations were slightly lower, they should still provide adequate resiliency for either aggregate type as indicated by the range of M_R values between 416 to 314 MPa and 390 to 327 Mpa, respectively.

Table 5.1 Summary of resilient modulus testing.

Aggregate Type	Gradation	Moisture Condition	Mean M_R (MPa)	Standard deviation
Glacially Derived	21AA	Dry	431.3	23.9
		Drained	414.6	39.9
		Undrained	139.6	11.7
	350AA	Dry	416.3	5.32
		Drained	369.8	30.3
		Undrained	153.5*	39.2*
	3G	Dry	389.7	29.0
		Drained	375.4	21.5
		Undrained	187.4*	60.0*
Quarried Limestone	21AA	Dry	431.5	24.4
		Drained	350.1	22.6
		Undrained	108**	**
	350AA	Dry	349.3	11.4
		Drained	313.7	13.9
		Undrained	***	***
	3G	Dry	368.5	18.6
		Drained	327.4	18.9
		Undrained	129.3	39.7

Note: All resilient modulus values are taken after step 11 as defined in Table 4.5. The * symbol indicates that 2 of the samples made it to step 11 before softening. ** Indicates 1 sample lasted until step 11. *** Indicates that no samples made it to step 11.

It is believed that the primary reason for the higher resilient response for the 21AA gradation is that its bulk density is greater than that of the 350AA and 3G gradations. Even though the 21AA gradations are compacted to only 95 to 96 percent of optimum, the bulk density was roughly 3 percent higher than the 350AA and 6 percent higher than the 3G (see Appendix K). Since the 21AA gradation was compacted to the highest bulk density, it has the smallest void ratio (the ratio of voids to the volume of solids) that translates to the greatest amount of particle on particle contact. This increased particle-to-particle contact within the sample increases the frictional strength of the aggregate. In dry cohesionless materials, the friction angle is an important factor in the resiliency. For example the 21AA glacially derived samples have a void ratio of roughly 0.24 while the 350AA and 3G are 0.30 and 0.35 respectively. This would correspond to friction angles being the greatest for the 21AA and least for the 3G. Increased friction angles directly relate to increased resiliency.

Calculated M_R values obtained for a given specimen at a given moisture condition were fit to the following power, linear regression model: $M_R = K_1 \theta^K_2$. The details of this analysis, including the values for both coefficients, are presented in Appendix K. Figure 5.1 shows a typical example of resilient modulus values versus bulk stress for a single specimen in the three different moisture conditions. Overall, the model fit for the dry and drained tests was good as indicated by the high correlation coefficient (R^2) values. The data obtained during undrained testing was more inconsistent, with lower R^2 values. This is not atypical for saturated materials. The results indicate that materials in an undrained condition are not only inconsistent but have also lost a majority of their resiliency. This is due primarily to the increased pore water pressure from the lack of drainage and 100 percent saturation.

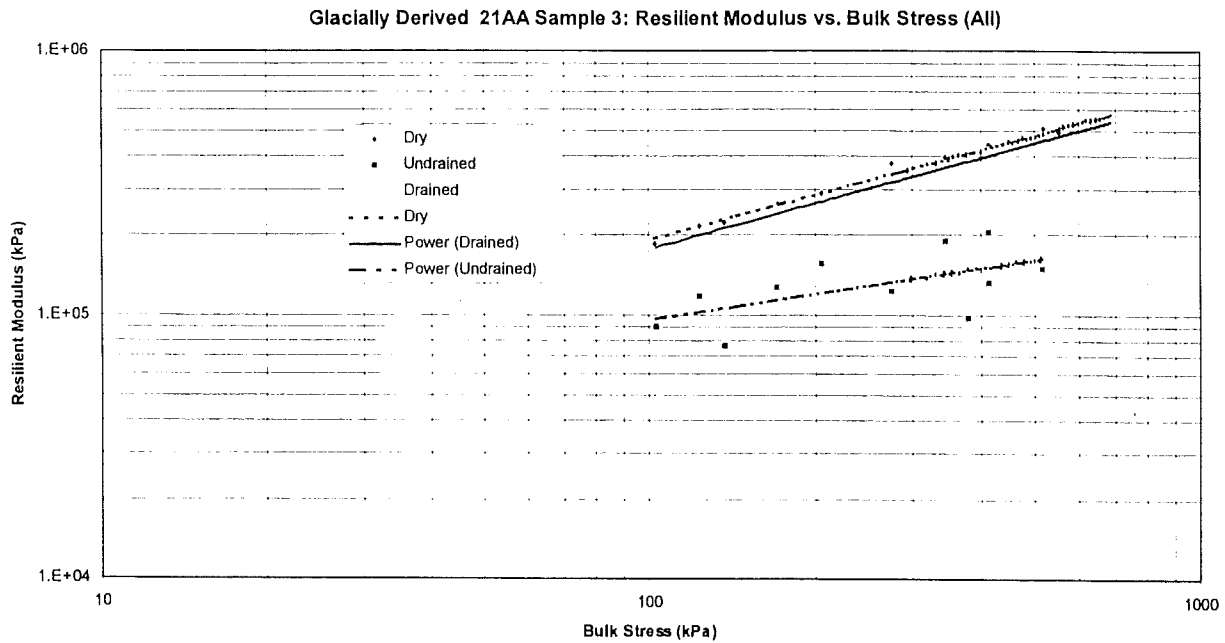


Figure 5.1. Resilient modulus versus bulk stress for glacially derived 21AA sample 3.

Comparing the mean M_R results for the three gradations in the various drainage conditions is very revealing. Although the overall differences are not great, there are some interesting trends as shown in Figures 5.2 and 5.3. It is noted that in all combinations of gradation and moisture condition, that the resiliency of specimens made with the glacially derived materials are higher than those made with the quarried limestone. This reflects the superior nature of that material which has undergone natural beneficiation through the grinding action of the glacier. It is suspected that if additional processing had not be used to create fractured faces on the particles, these results would not have been obtained.

Resilient Modulus vs. Moisture Condition for Glacially Derived Material

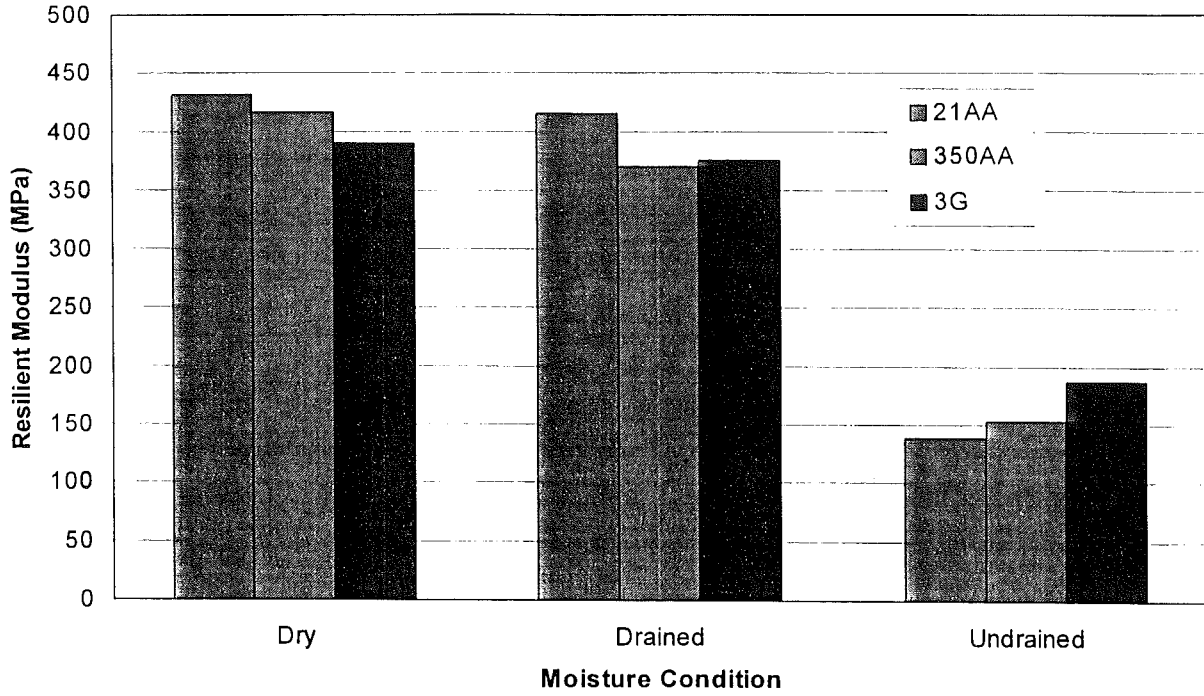


Figure 5.2 Resilient modulus versus moisture condition for glacially derived materials.

Resilient Modulus vs. Moisture Condition for Limestone Material

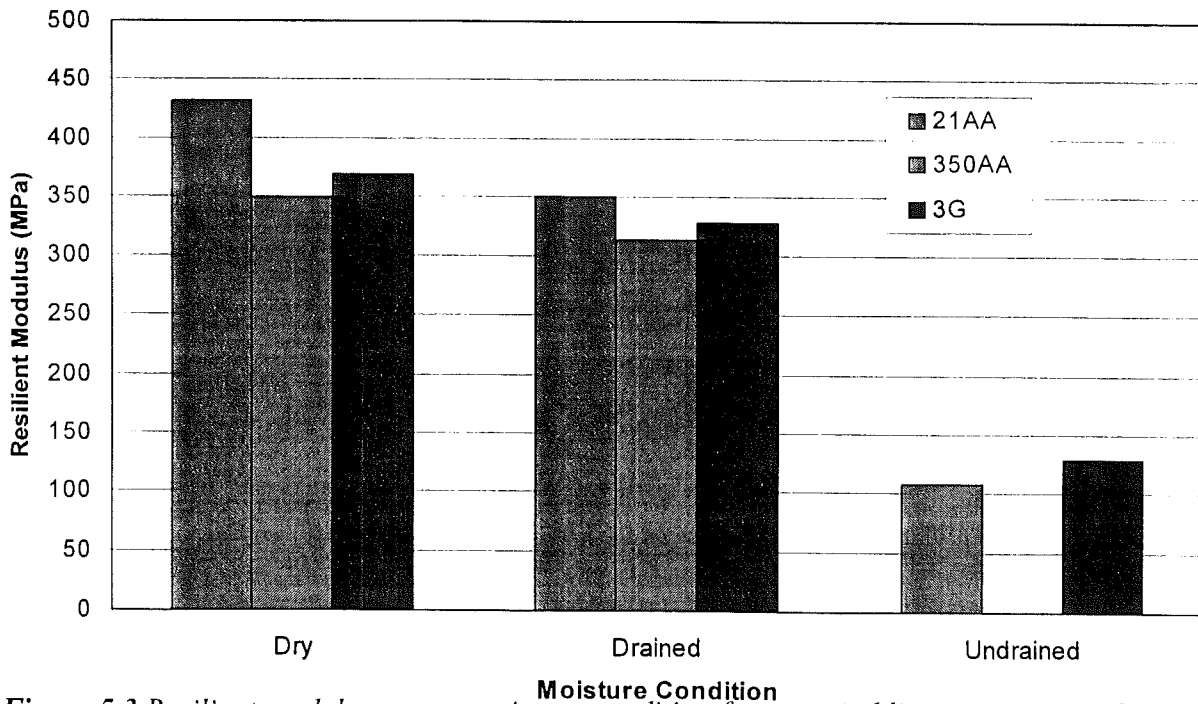


Figure 5.3 Resilient modulus versus moisture condition for quarried limestone materials.

Also, within any given material, it is observed that the 3G gradation has the lowest

resiliency in the dry condition whereas the 21AA are the most resilient. The 21AA specimens remain the most resilient in the drained condition, but specimens made with the 3G gradation surpass the resiliency of those made with the 350AA. And in undrained condition, the 3G gradation is the most resilient whereas the 21AA has the lowest resiliency.

Another important piece of information obtained from this testing is the permanent deformation characteristics of the various materials under repeated dynamic loading. A summary of these results is presented in Table 5.2 and detailed information is provided in the Appendix. Figure 5.4 is a typical plot of the deformation data collected, with additional plots provided in the Appendix. It is observed that a marked difference in permanent deformation characteristics was observed between the three gradations. The material showing the least permanent deformation (0.72mm) through the drained test was the glacially derived 21AA. This was followed closely by the specimens made with the 3G gradation (both glacially derived and quarried limestone) which had an average permanent deformation of 0.86mm at the end of the dry condition testing. The 350AA gradation (both glacially derived and quarried limestone) had the most permanent deformation at 1.1mm at the end of the dry condition testing. It is noted that the 3G gradation made with the quarried limestone material appears to provide adequate resistance to permanent deformation well into the undrained portion of the testing sequences. Comparatively, the glacially derived 3G curve depicts a random trend, suffering excessive deformation earlier in the testing sequence than the quarried limestone material. Both dense graded (21AA) materials display inconsistent trends and excessively deform very rapidly during the undrained test.

The most surprising result is that the 350AA gradation displayed the highest amount of permanent deformation for all phases of the testing sequence. This occurred even though all of the 350AA samples were compacted to at least 97 percent of optimum density. The occurrence of relatively high permanent deformation early in the testing sequence for the 350AA gradation is disturbing. The results of the study are statistically inconclusive because of the limited number of tests conducted in light of the variability between tests. But there is enough concern in this preliminary work to warrant additional investigations before the 350AA is adopted as a standard base course gradation.

The primary reason for performing the resilient modulus testing was to measure the response to dynamic loading of typical MDOT gradations under the three moisture

conditions. In the past it was common practice to place a PCC pavement onto a 21AA base course without a drainage system. It is suspected that such base courses are at or near an undrained, saturated condition for most of their lifetime in the field. For example, assume that a 300-mm thick base (much thicker than the typical 100-mm thick base) is used on a 4-lane pavement drained to either side. The hydraulic gradient is 0.03 and the drainage distance is half the pavement width at 10 meters. Also assume that the flow through the base course obeys Darcy's law (laminar flow) and that there is 50 mm of rain falls on the pavement structure and 35 percent infiltrates the base course. Using the approach advocated by Cedergren (from Cedergren, H.R, "Drainage of Highway and Airfield Pavements", pages 75 – 87), a 21AA material having a calculated coefficient of permeability (k) of roughly 0.3 m/day will take roughly 700 hours to drain to an unsaturated state. Using the same assumptions, a 350AA (k = 110 m/day) or a 3G (k = 300 m/day) base course connected to a functioning drainage system will drain in 5.5 hours or 1 hour, respectively. This is 200 to 700 times faster than the base course constructed with a 21AA. So for similar rain events, the base constructed on a 21AA base course will remain in a saturated condition for significantly longer than the bases constructed of 350AA or 3G materials.

Table 5.2 Summary of permanent deformation results.

Aggregate Type	Gradation	Mean Deformation @ end of Dry test (mm)	Mean Deformation @ end of Drained test (mm)	Mean Step # @ 2mm Deformation Undrained	Range of Step #'s
Glacially derived	21AA	0.428	0.72	Step 15	None
	350AA	0.71	1.1	Step 13	9 – 15
	3G	0.527	0.86	Step 12	9 – 15
Quarried limestone	21AA	0.507	0.975	Step 10	9 – 12
	350AA	0.581	1.1	Step 9	8 – 9
	3G	0.49	0.86	Step 15	none

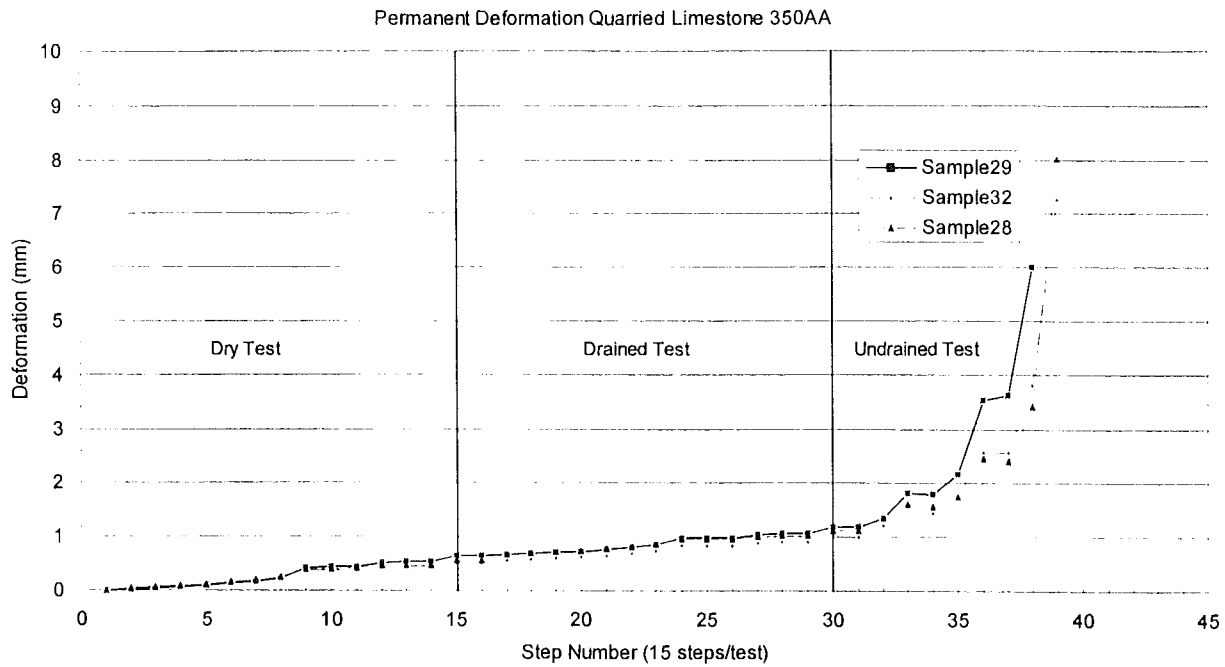


Figure 5.4 Permanent deformation recorded for quarried limestone 350AA.

Currently, drainage systems are installed in all new Portland Cement Concrete (PCC) pavements in Michigan. If routine maintenance is performed, the drainage systems should provide adequate drainage for the PCC pavements constructed with draining base materials for its entire design life, minimizing the time that an undrained condition occurs. The example above shows the importance of a properly functioning drainage system. It illustrates that a drainable base system will be in a saturated condition following a rain event for only a short period of time. On the other hand, a 21AA base course will remain at or near saturation roughly 700 times longer than the 3G material. During this time the 21AA material will experience more permanent deformation and a dramatic decrease in resiliency.

But if maintenance of the drainage system is neglected, it may become clogged, therefore creating an undrained or saturated condition. The information shown in Tables 5.1 and 5.2 clearly indicates that all base materials in the undrained state will experience a dramatic decrease in resiliency and an increase in the permanent deformation. Increases in permanent deformation create voids beneath the PCC slab and may lead to an array of premature pavement failures.

The results from the undrained tests clearly indicate a significant decline in the resilient modulus (M_R) and K_2 coefficient (slope), while the K_1 coefficient increases very sharply. This decrease in the M_R values is directly related to the pore water pressure (u) being generated in the saturated sample. Therefore, the effective stress (σ') within a sample decreases if pore pressure increases according to: $\sigma' = \sigma_1 - u$, where $\sigma_1 =$ principle stress ($\sigma_d + \sigma_3$) and u is the pore water pressure. Therefore as u increases the effective stress, σ' decreases. At a saturation (S) of 100%, in undrained conditions the pore pressure will equal the confining stress σ_3 , $u = \sigma_3$, as shown in Table 4.5. This would indicate that the sample is limited to effective stress and will be susceptible to any vertical stress applied. If undrained conditions exist in the field due to a clogged drain, the base course material will not provide adequate resiliency or resistance to deformation for normal conditions since pore pressure developed. This is evident in the M_R values as well as the permanent deformation charts.

In conclusion, the data indicates that if drainage is present, both types of aggregate and all the three gradations should provide adequate support for a PCC slab under typical loading conditions. But, it is noted that the 21AA base will be in a saturated undrained condition for much of the time even if a positive drainage system is provided because its time to drain is very long. This will likely cause pavement damage due to the material's loss in resiliency and susceptibility to permanent deformation. Timely maintenance is needed to prevent clogging of drainage systems when drainable materials are used. If clogging occurs, an undrained or saturated condition will exist, dramatically decreasing the resiliency and increasing the amount of permanent deformation for all materials and gradations. This can result in void formation under the PCC slab that could lead to a host of structural failures. Both the 21AA and 3G gradations displayed high resiliency with small deformations for the dry and drained tests. For the materials and gradations under investigation, the undrained test clearly shows that the quarried limestone 3G gradation displayed consistent strength and low deformation in the undrained tests. There is concern that the 350AA gradation may be more susceptible to permanent deformation than the other two gradations and further testing is recommended.

5.2 Effect Of Drainage On AASHTO Rigid Pavement Thickness Design

Thickness design for rigid pavements is commonly conducted using the procedures described by AASHTO in the *AASHTO Guide for Design of Pavement Structures* (AASHTO 1993). The design procedures are based on the results of the AASHTO Road Test conducted from 1958 to 1960 in Ottawa, Illinois. Modifications to this procedure have been made over the years to incorporate additional design parameters and improve its applicability over a wide geographical area.

5.2.1 The AASHTO Thickness Design Procedure

The 1986 version of the design procedure is the most current, appearing again in the 1993 design guide. Slab thickness is determined by solving the following equation:

$$\log_{10}(W_{18}) = Z_R S_0 + 7.35 \log_{10}(D+1) - 0.06 + \frac{\log_{10} \left[\frac{\Delta PSI}{4.5 - 1.5} \right]}{1 + \frac{1.625 * 10^7}{(D+1)^{8.46}}}$$

$$+ (4.22 - 0.32 p_t) * \log_{10} \left[\frac{S'_c * C_d [D^{0.75} - 1.132]}{215.63 J \left[D^{0.75} - 18.42 \left(\frac{k}{E_c} \right)^{0.25} \right]} \right]$$

Where:

W_{18} is the number of 80-kN (18-kip) equivalent single axle loads.

Z_R is the standard normal deviate corresponding to the selected reliability level.

S_0 is the overall standard deviation.

D is the thickness of the PCC slab, in.

ΔPSI is the design serviceability loss.

p_t is the design terminal serviceability.

S'_c is the 28-day PCC modulus of rupture, psi.

J is the load transfer coefficient.

C_d is the drainage coefficient.

E_c is the 28-day PCC modulus of elasticity, psi.

k is the modulus of subgrade reaction, psi/in

The design equivalent single axle loads (W_{18} or ESALs) are calculated from the volume and type of traffic anticipated over the pavement design life. The selected reliability level depends on the functional classification of the pavement structure, with more heavily trafficked pavements requiring higher reliability levels. For example, a low volume rural roadway may be designed with a reliability level ranging from 50% to 80% while an urban interstate may demand 85% to 99.9% reliability. The overall standard deviation is usually assumed to lie between 0.34 and 0.39 for rigid pavements, depending on whether traffic error is included in the estimation.

The entire AASHTO pavement design is based on the serviceability concept as measured using the present serviceability index (PSI). A pavement in perfect condition (and perfectly smooth) will have a PSI approaching 5 whereas a completely impassable, very rough pavement will have a PSI approaching 0 (zero). The most influential factor affecting PSI is the roughness of the pavement, and therefore many consider roughness and PSI to be synonymous. In new PCC construction, an initial PSI (p_i) of 4.5 is commonly assumed based on construction at the AASHTO Road Test. This appears to be a reasonable estimate when modern construction techniques and roughness specifications are used. The selected design terminal serviceability (p_t) will depend on the functional classification of the pavement, typically ranging between 2.5 and 3.0 for major highways. In the following discussion, pavement failure is considered the point at which terminal serviceability is reached.

Material properties are incorporated in three parameters: the 28-day PCC modulus of rupture (S'_c), the 28-day PCC modulus of elasticity (E_c), and the effective subgrade modulus of rupture (k). The two concrete properties are based on laboratory testing of the concrete mix design or estimated based on specified concrete properties.

The subgrade modulus of rupture can be estimated from soil properties or established through field-testing. NDT can also be used to determine the k -value supporting an existing slab, but must be reduced by a factor of two to convert from dynamic to static loading. It is noted that an "effective" k -value is used in the AASHTO design procedure, having been corrected for climatic variations, the stiffness and thickness of the subbase, the depth to bedrock, and the loss of support that can result from erosion of the subbase. The quality and drainability of the subbase is thus considered in the effective k -value, especially in selecting the loss of support factor (LS). For untreated granular material, it

is recommended that an LS of 1 to 3 be used. This will significantly reduce the design k-value. In the example presented in the design guide, a k-value of 540 psi/in is reduced to 170 psi/in when an LS of 1 is used and to 20 psi/in when an LS of 3 is used.

Although drainage is indirectly incorporated through modification to the k-value, it is directly considered in design through the drainage coefficient (C_d). Two factors are considered in determining the C_d : the quality of the subbase drainage and the percent of time the pavement structure remains in a saturated state. Table 5.3 below provides recommended values for C_d for use in rigid pavement design.

Table 5.3 Recommended values for the drainage coefficient, C_d (AASHTO, 1993).

Quality of Drainage	Percent Of Time Pavement Structure Is Exposed To Moisture Levels Approaching Saturation			
	Less than 1%	1%-5%	5%-25%	Greater than 25%
Excellent	1.25-1.20	1.20-1.15	1.15-1.10	1.10
Good	1.20-1.15	1.15-1.10	1.10-1.00	1.00
Fair	1.15-1.10	1.10-1.00	1.00-0.90	0.90
Poor	1.10-1.00	1.00-0.90	0.90-0.80	0.80
Very Poor	1.00-0.90	0.90-0.80	0.80-0.70	0.70

Quality of drainage is based on the time required to drain the subbase to 50 percent saturation. A pavement structure with excellent drainage quality will achieve this within two hours of cessation of the precipitation event. If 50 percent saturation occurs within one day, the drainage quality is considered good and if it takes one week, fair drainage exists. Poor drainage quality exists if it takes one month to achieve 50 percent saturation. If the subbase is non-draining, it is considered to have very poor quality drainage.

The ability of a material to drain is primarily related to the amount and type of fine material present. As the amount of fines increases, drainage quality decreases. Further, the presence of inert mineral fillers will have far less impact on drainability than clays. Table 5.4 below presents the amount of water that can be drained from saturated gravel or sand under gravity for various contents and types of fines. As can be seen, once a material having more than 5 percent fine material becomes saturated, it is unable to achieve 50 percent saturation under gravity alone.

Table 5.4 Estimate of the amount of water that can be drained from saturated granular materials under gravity (ERES 1994).

Material	Amount of Fines								
	<2.5 percent			5 percent			10 percent		
	Filler	Silt	Clay	Filler	Silt	Clay	Filler	Silt	Clay
Gravel	70	60	40	60	40	20	40	30	10
Sand	57	50	35	50	35	15	25	18	8

Note: Gravel with 0 percent fines, 75 percent greater than No. 4: 80 percent water loss.

Sand with 0 percent fines, well graded: 65 percent water loss.

The final design parameter in the PCC thickness design equation is the load transfer coefficient, *J*. This factor considers the pavement type, the type of shoulder, and the type of load transfer devices present. Poor load transfer conditions, such as exists in jointed, undoweled pavements with asphalt concrete shoulders will have high load transfer coefficients on the order of 3.8 to 4.4. A concrete pavement constructed with tied concrete shoulders and dowels at the transverse joints will have lower load transfer coefficients in the range of 2.5 to 3.1.

5.2.2 Evaluation of the Effect of Drainage on Pavement Design Life

The AASHTO design procedure was used to assess how the drainage characteristics of the pavement system would affect the expected pavement performance. As described above, drainage will directly influence two parameters in the design equation: the effective modulus of subgrade reaction (*k*) and the drainage coefficient (*C_d*). Using the information obtained through coring and NDT analysis, representative baseline, minimum, and maximum values were established for the sections under investigation in this study. These are presented in Table 5.5.

Table 5.5 Range in AASHTO design parameters used to assess the affect of drainage on concrete pavement performance.

Parameter	Baseline	Minimum	Maximum
PCC Modulus of Rupture, S'_c	640 psi	600 psi	680 psi
Effective Modulus of Subgrade Reaction, k	150 psi/in	50 psi/in	200 psi/in
Load Transfer Coefficient, J	3	3	4
Drainage Coefficient, C_d	1.0	0.7	1.25

Pavement thickness was varied from 230 mm to 305 mm (9 to 12 inches). Reliability was set at 95% and the overall standard deviation was assumed to be 0.39. The initial and terminal PSI were assumed to be 4.5 and 2.5, respectively.

The AASHTO design equation was used to predict design ESALs for each pavement thickness and combination of variables. Thus, the predicted ESALs to terminal serviceability is the measure of performance considered. The results of this analysis are tabulated in Tables 5.6 through 5.9.

It is readily observable that thickness is a very important consideration. As slab thickness is increased from 230 mm to 305 mm, the design ESALs increases from 2.25 million to 15.0 million for the baseline values for each parameter. For a given slab thickness, it is observed that the design ESALs varies significantly from the worst to the best case scenario. For example, the design ESALs varies from 0.35 million to 12.25 million for a 255 mm thick slab.

As mentioned, the range in values for the variables considered was estimated from data collected in the course of this study. In examining the effect of each individual parameter on expected performance, it is observed that changes in the modulus of rupture, the modulus of subgrade reaction, and the load transfer coefficient have relatively little effect on expected performance over the ranges considered. Typically, design ESALs are roughly doubled or tripled from the worst case to the best case for these variables.

On the other hand, the drainage coefficient is observed to have a very large impact, with design ESALs varying by more than six times over the range of the variable. This coefficient reflects the quality of drainage of the subbase material as well as the climatic

Table 5.6 Predicted design ESALs for 230 mm PCC pavement using the AASHTO design equation.

Variable	Range of Values	ESALs (millions)
Modulus of Rupture (S'_c)	600 psi	2
	*640 psi	2.25
	680 psi	3.0
Effective Subgrade Modulus (k)	50 psi	1.75
	100 psi/in	2
	*150 psi/in	2.25
	200 psi/in	2.5
Load Transfer Coefficient (J)	4.0	0.9
	3.5	1.4
	*3.0	2.25
Drainage Coefficient (C_d)	0.7	0.7
	*1.0	2.25
	1.25	4.75
Worst Case	Lowest value for each variable	0.17
Baseline Pavement Conditions	Baseline using the * values	2.25
Best Case	Highest value for each variable	6.45

Table 5.7 Predicted design ESALs for 255 mm PCC pavement using the AASHTO design equation.

Variable	Range of Values	ESALs (millions)
Modulus of Rupture (S'_c)	600 psi	3.5
	*640 psi	4.5
	680 psi	5.5
Effective Subgrade Modulus (k)	50 psi/in	3.5
	100 psi/in	4.25
	*150 psi/in	4.5
	200 psi/in	5.0
Load Transfer Coefficient (J)	4.0	1.75
	3.5	2.75
	*3.0	4.5
Drainage Coefficient (C_d)	0.7	1.4
	*1.0	4.5
	1.25	9.25
Worst Case	Lowest value for each variable	0.35
Baseline Pavement Conditions	Baseline using the * values	4.5
Best Case	Highest value for each variable	12.25

Table 5.8 Predicted design ESALs for 280 mm PCC pavement using the AASHTO design equation.

Variable	Range of Values	ESALs (millions)
Modulus of Rupture (S'_c)	600 psi	6.75
	*640 psi	8.25
	680 psi	10.0
Effective Subgrade Modulus (k)	50 psi/in	6.5
	100 psi/in	7.5
	*150 psi/in	8.25
	200 psi/in	9.0
Load Transfer Coefficient (J)	4.0	3.25
	3.5	5.0
	*3.0	8.25
Drainage Coefficient (C_d)	0.7	2.6
	*1.0	8.25
	1.25	17.0
Worst Case	Lowest value for each variable	0.65
Baseline Pavement Conditions	Baseline using the * values	8.25
Best Case	Highest value for each variable	22.5

Table 5.9 Predicted design ESALs for 305 mm PCC pavement using the AASHTO design equation.

Variable	Range of Values	ESALs (millions)
Modulus of Rupture (S'_c)	600 psi	12.0
	*640 psi	15.0
	680 psi	17.5
Effective Subgrade Modulus (k)	50 psi/in	11.75
	100 psi/in	13.25
	*150 psi/in	15.0
	200 psi/in	15.5
Load Transfer Coefficient (J)	4.0	5.75
	3.5	9.0
	*3.0	15.0
Drainage Coefficient (C_d)	0.7	4.75
	*1.0	15.0
	1.25	30.0
Worst Case	Lowest value for each variable	1.2
Baseline Pavement Conditions	Baseline using the * values	15.0
Best Case	Highest value for each variable	40.0

conditions that can lead to saturation. Overall, Michigan has a wet climate and precipitation is such that sufficient quantities of moisture are available to keep a non-draining base at or near saturation year round. Thus the drainage coefficient will be wholly dependent on the quality of the drainage. A dense graded base with fines in excess of 5 percent will be very slow draining. According to AASHTO procedures, a drainage coefficient in the range of 0.70 to 0.80 would be appropriate for this type of material. On the other hand, an open graded drainable base connected to a drainage system would be assigned a drainage coefficient in the range of 1.20 to 1.25. The difference in this change in the drainage coefficient is roughly equivalent to changing the PCC thickness from 230 mm to 305 mm according to this analysis.

Thus, in designing a PCC section with a drainable base, a relatively high value for the drainage coefficient will be selected. This will result in the design of a thinner slab than if a non-draining dense-graded subbase was used. If the drainage system is improperly designed, constructed, or maintained, resulting in long periods of saturation, the thinner slab would be expected to fail much more quickly than anticipated. For example, based on this design method, a 230 mm thick slab designed for 17.0 million ESALs assuming excellent drainage would be expected to fail within 2.6 million ESALs if very poor drainage was actually achieved.

6. ANALYSIS OF TEST SECTIONS

6.1 Evaluation of Michigan Pavement Distress Levels With Respect to the LTPP Database

In order to qualify the distress levels observed at each test section, it was necessary to identify a reference system. Such a reference was found in the Federal Highway Administration's (FHWA) "Long-Term Pavement Performance" (LTPP) database containing information on JRCP throughout The United States and Canada. The database was compiled by Soils and Materials Engineers (SME) for FHWA's "Study to Investigate the Factors Effecting the Development of Roughness in Pavements," and was expanded by the U of M research team. From the LTPP database it was possible to extract distress levels for pavements that are similar to those studied in this project. This was done for JRCP sections in the wet-freeze climate region with slab lengths ranging from 30 to 50 ft. The latter was considered comparable with the average 41 ft slab length in Michigan. 16 pavements were found to meet the above requirements. Figure 6.1 shows the approximate locations of those pavements.

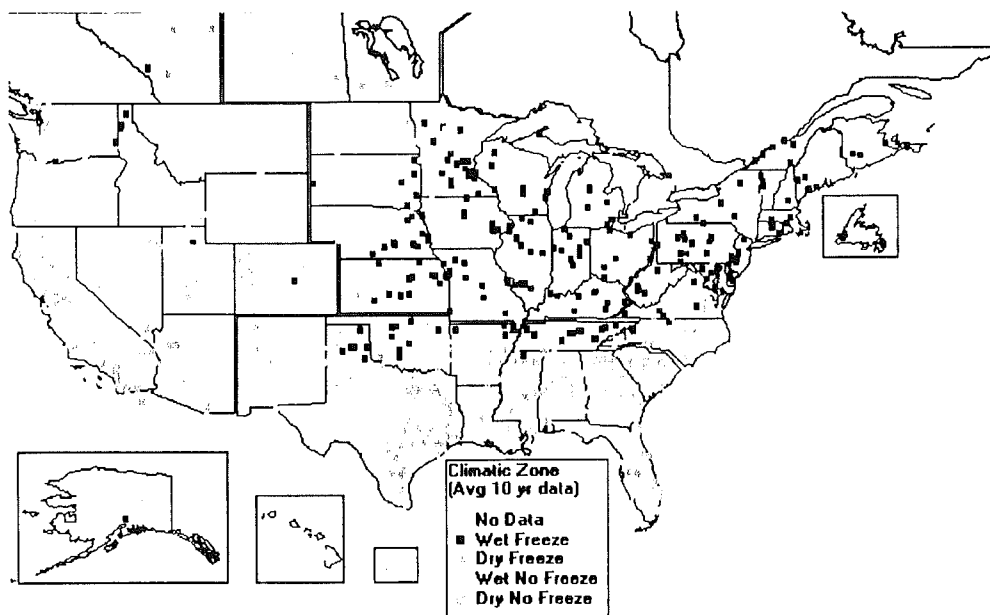


Figure 6.1 Approximate location of the LTPP pavements in wet/freeze region

Explain better

Development of transverse cracking and spalling was plotted for each of these sections using dimensionless unit "L/L", or total length of distress (ft), per slab length (ft). A similar calculation was performed for spalling. Average faulting was also determined. Table 6.1 lists the age at time of testing along with the calculated dimensionless distress indices from field measurements for each of the test sections in this study. The last column in Table 6.1 categorizes the overall distress level in terms of low, medium and high distress.

Table 6.1 Dimensionless distress index for transverse cracking, spalling as deteriorated length divided by total length of section. Average faulting is also indicated. The overall classification of the overall distress level is indicated as low, medium, and high.

point spacing varies - Fracture adjusted for this

How was length measured vs width?

Incomplete?

Test Section	Age	Spalling	Transverse Cracking	Faulting per 500 ft ave fault (mm)	Distress Category
		LL	LL		
19042-02233A Sec C	9	0.0056	0.6328		
19042-24680A Sec B	10	0.0038	0.0714		
19043-02234A EB	11	0.0031	0.4854		
19043-02234A WB	11	0.0000	0.2570		
44044-18804A	12	0.0262	0.5396		
77024-20821A Sec A	13	0.0708	0.6074		
77024-17988A Sec B	12	0.0004	0.5424		
25132-06582A	16	0.0010	0.3009	-0.04	
77023-21586A	13	> 0.0500	0.7941	-1.21	
11017-32516A Sec A	2	0.0007	0.4379		
11017-32516A Sec C	2	0.0000	0.0485	-0.32	
11017-32516A Sec D	1	0.0000	0.0475		

Negative # how many faulted cracks?

Figures 6.2 and 6.3 show the dimensionless distress (transverse cracking and spalling respectively) vs. age for both the LTPP sections and the sections tested in this study. These results show that the average value of transverse cracking is more pronounced for the 8 OGDC and 3 DGBC sections studied along I-69 and I-475 than those in the LTPP database of similar age and slab length, and within the same climatic (wet-freeze) zone. However, the average spalling index is lower for most sections as compared to the LTPP data base. The sections exhibiting high spalling index are 77024-20821 Sec A, 77023-21586A and 44044-18804A. Spalling of a crack is a major concern since it requires rehabilitation such as patching.

By just looking?

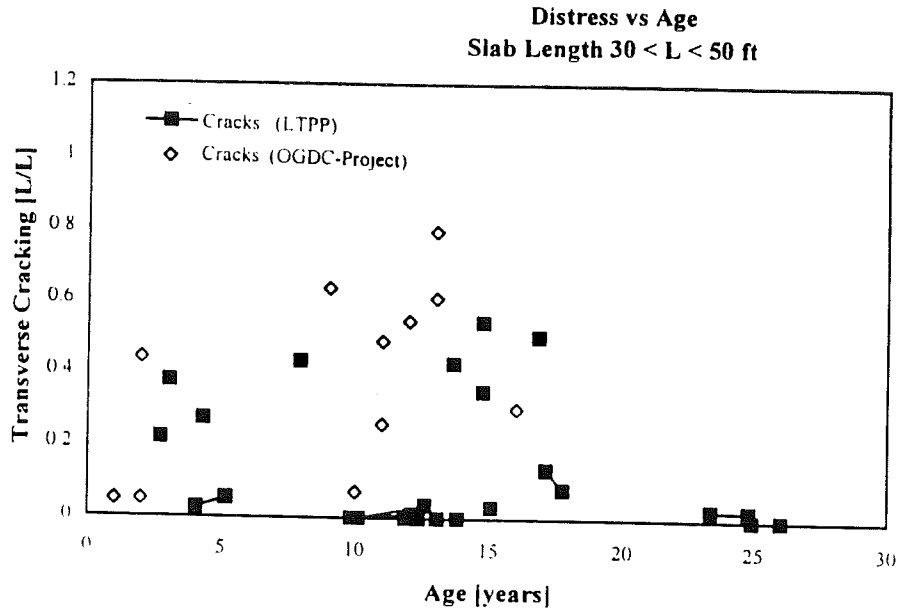


Figure 6.2 Dimensionless transverse cracking distress index vs. age for the Michigan test sections and similar sections in the LTPP database.

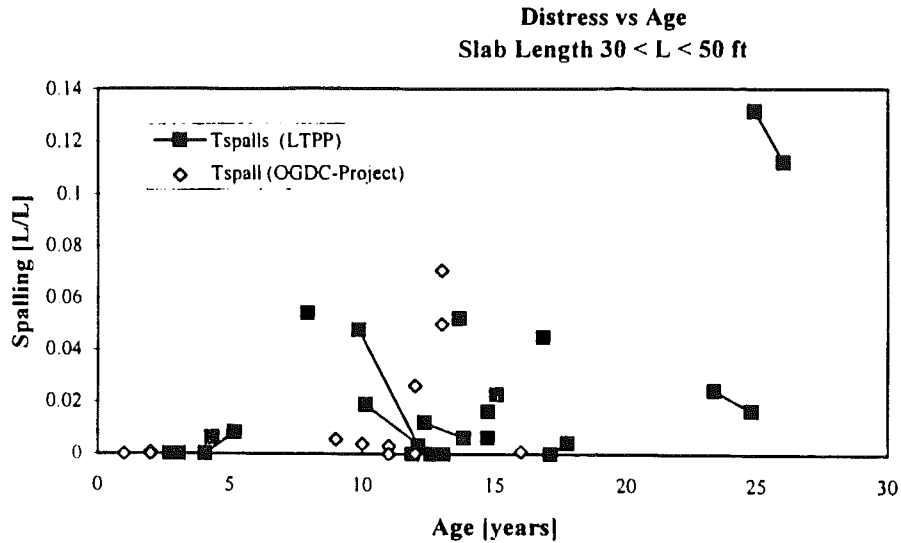


Figure 6.3 Dimensionless spalling distress index vs. age for the Michigan test sections and similar sections in the LTPP database.

The higher than expected degree of transverse cracking among the Michigan sections may be attributed to the sympathy cracking problem for the sections containing intermediate PCC shoulder joints with three panels per PCC slab. This design has been known to initiate cracking in the slab near the third point. For pavements above 10 years of age, it

seems to indicate that $L/L > 0.6$ is a critical threshold. This indicates that the sections 19042-02233A (Section C), 77024-20821 (Section A) and 77023-21586A have a disturbingly high level of transverse cracking. These sections in particular deserve further consideration.

It is also, however worthwhile to look at new pavements that are experiencing early distress. Several OGDC pavement projects have been studied which have shown a high degree of transverse cracking within the first few months to a year after construction. They include 11017-32516, sections A and C, eastbound on I-94 near Watervliet, and northbound US-23 south of Dundee. These are JPCP's with 16 ft slab lengths and JRCR with 27 ft slab length respectively. The commonality between these projects is that they were both constructed in hot weather with PCC placement temperatures in the mid-to upper eighties, and they have same base gradations (3G crushed). The causes of this early distress will also be evaluated further in the next sections.

6.2 Major Causes for the Deterioration of the Michigan Study Sections

6.2.1 Drainage Issues

Pumping

Three of the poorest performing sections among the OGDC pavements studied were found to have distress associated with pumping. The pumping in turn had resulted in excessive transverse crack and joint faulting. These sections were 44044-18804A in Lapeer County, and sections 77023-21586A and 77024-20821A in St. Clair County. The two Lapeer County sections were found to have clogged edge-drain outlets and poor drainage.

By contrast, another job within the same control section, 77024-17988A, has performed well under similar traffic and environmental conditions. The good performing 77024-17988A has an 18 inch subbase of clean sand and a crushed gravel base material, whereas the poorer 77024-20821A has untreated natural aggregate base on an 8 inch subbase over clay subgrade with very high fines content ($P_{200} = 76\%$). For the good performer, outlet drains were clean, indicating that little or no erosion of subbase or subgrade fines. The apparent reason why 77024-17988A performed much better, even though it also had a subgrade with high fines content ($P_{200} = 53\%$), was that the thick subbase greatly reduced the pumping action at the subbase-subgrade interface. Without pumping, the

subgrade fines were not eroded into the drainage structure. It is expected that once water became trapped because of clogged drains in the 77024-20821A section, pumping was magnified, and foundation support was quickly lost. This was evidenced by faulting of approximately 0.25 inch. Furthermore, the faulted cracks have become severely spalled, indicating large deflections of the pavement under truck loading.

Reduced base support related to permanent high moisture content is clearly evident from resilient modulus testing, as will be described later in detail. Appendix K contains the resilient modulus data.

The bottom line of the comparison is that inadequate subbase thickness can cause erosion of the subgrade, clogged drains, and increased deterioration of transverse cracks such as faulting and spalling. It should be noted that the concrete properties have been ruled out as a cause for the distress, further implicating the large slab movements in the spalling behavior of the cracks.

Base-Subbase Compatibility

While in most cases the OGDC has improved drainage underneath the slab and thus prevented rapid distress due to high trapped moisture content (typically associated with DGBC's), the compatibility between the base and subbase is more critical for OGDC pavements.

Because the open structure of the OGDC base allows water to pass through rapidly, this leaves the subbase more exposed to high water velocities and pumping under saturated conditions. In other words, the same subbase materials that are compatible with dense graded bases courses may be incompatible with an OGDC layer. Therefore, the percentage of fines in the subbase are also critical in an OGDC system, which can be supported by test section 77023-21586A, where the subbase is found to contain 17% fines passing the #200 sieve. The high P200 of the subbase reduces the permeability tremendously, and causing the base layer to be in a undrained condition for a longer time after a rainfall event. As will also be discussed in the resilient modulus testing section, the permanent deformations of a base material are 7 to 10 times higher in undrained conditions than in drained conditions. The later causes permanent settlements of base course near joints and cracks, erosion of subbase, faulting and clogging of drainage structures.

It is surprising to note that the best performing OGDC sections 19042B-24680A, 77024-17988A, 19042C-02233A, all violate, at least to some degree, the filter criteria between base and subbase. On the other hand, these sections all have a thick sand embankment or a sandy subgrade. This again leads to the conclusion that increased the layer thickness above erodible layers will help to ensure that the water either runs into the drains before it meets the erodible layers, or the pumping pressures are sufficiently damped to avoid erosion. The above statement is also valid for the DGBC sections 19043-02234A westbound and eastbound.

Frost Susceptibility

Returning to the subbase, it was stated earlier that the subbase on 77023-21586A contained 17% fines passing the #200 sieve. Such a fine material is susceptible to frost heave due to increased capillarity. While statements to that effect could not be found in the construction records for this section, the records for section 44044-18804A indicated several locations where frost heave had been observed. The construction records also indicate that swamp backfill treatment was used at several locations. Whether, that test section's faulted and spalled transverse cracks were due to silt pockets and associated frost heave in the subgrade or due to inadequate drainage could not be determined. It is noted that plastic limit and liquid limit were not determined for the studied foundation materials.

What point is being made?

6.2.2 Slab Rocking and Thermal Effects

Slab Rocking

In a study by Poblete, transverse cracking was observed at midslab in plain and undoweled newer pavements within the first three years after placement. These pavements showed perceptible rocking of short slabs under early morning conditions. Furthermore, the pavements had no signs of pumping and drainage problems. And cracking started at midslab from the longitudinal edges, and propagated from the top downward and toward the slab interior. The condition illustrated by Poblete describes in detail the phenomena observed on I-94 near Watervliet (11017-32516A, sections A and C). Similar distress had been noted on US-23 south of Dundee two years earlier.

Perceptible rocking was found over the joints and cracks for sections 11017-32516A A and C for morning conditions under truck loading. This observation suggests an upward curled slab. This has been verified through Falling Weight Deflectometer (FWD) testing

at joints and cracks during morning and afternoon conditions. Morning deflections were higher at edges and joints than in the afternoon, and were accompanied a small but measurable uplift of the slab from the foundation (2-4 mils). Figures 6.4 and 6.5 are typical of morning and afternoon load-deflection results for these test sections. Higher slab temperatures during afternoon conditions are associated with a flatter slab, indicating that the rocking phenomenon is related to through thickness temperature gradients in the slab. Furthermore, it has been seen that rocking is exacerbated by high temperature placing. This condition was especially pronounced in slag concretes placed during summer weather and in short slabs such as the 11017-32516A and 47065-28215A eastbound on I-96 near Howell.

This figure will be added in the final report

Figure 6.4 Morning load-deflection results for 11017-32516A sections A and C.

This figure will be added in the final report

Figure 6.5 Afternoon load-deflection results for 11017-32516A sections A and C.

As was observed in two papers by the U of M research team (Hansen et al., 1997; Mohr et al., 1997), the time of day of placement can have considerable impact on the stress development within the slab. Early morning placements on a hot summer day lead to a maximum heat development at roughly the same time as the maximum daily temperature, leading to significant curling and contraction of the slab as it cools. This in turn leads to high built in stresses. This effect is corroborated by comments in the historical records for the 11017-32516A sections that indicate that cracking was most severe in the areas placed during the morning.

Base friction

It has been observed that OGDC base types may result in higher than expected slab friction at the slab base interface. This may further contribute to early midslab cracking associated with high temperature PCC slab placement conditions, which also cause high degree of slab contraction upon cooling. It was noticed that all OGDC cores have approximately a 1 inch rough bottom surface layer of bonded aggregate from penetration of the fresh mortar into the open layer structure of the OGDC. Cores obtained from DGBC sites all had a well defined smooth surface at the slab-base interface which indicates that no penetration of the mortar into the base. This is illustrated in Figure 6.6 which shows typical interfaces for the OGDC and DGBC sections.

This figure will be added in the final report

Figure 6.6 *Concrete-base interface of OGDC and DGBC core samples*

If OGDC pavements indeed have high degree of slab-base friction it would also help explain why pavements placed in cooler weather (early spring) at PCC placement temperatures below 70°F are performing very well. The frictional restraint of this interface would then place the slab in compression during higher temperatures in the summertime. The OGDC sections, whose good performance would be well explained by this phenomenon are 19042-24680 section B, 77024-17988 section B, and 11017-32516A section D.

The down side is that the built-in tensile stresses are maximum at mid-slabs for PCC slabs placed in hot weather conditions. These slabs are in tension all the time, until stresses are released from mid-slab cracking, since the internal PCC temperature at time of set was well over 100 F. Furthermore, tension in the slab associated with cold fall and winter temperatures can be even more severe for these same slabs. It is interesting to note that cracking on US-23 was first observed in October, after temperatures had dropped.

6.2.3 Crack Spalling

A section will be added here in the final report discussing the crack spalling problem. Also included here will be a discussion of how the load transfer efficiency LTE vs. crack width relation can be used to help in deciding when aggregate interlock is lost, and when a working crack has formed, and resulting spalling can be expected.

6.3 RQI as a Measure of OGDC vs. DGBC Pavement Distress Development

Included in Appendix F is a database of information on ride quality index (RQI) for OGDC and DGBC pavements which were constructed near the transition period from one base type to another. RQI, which is a measure of surface roughness of the pavement, is related to pavement distress development. The data presents the average RQI, standard deviation of RQI, and the annual growth rate of RQI for the various construction contracts. 36 separate sections were reviewed. Each traffic direction within a contract was treated as a separate section. This analysis is based on the 1992 through 1995 RQI data.

The information contained in the RQI database is shown graphically in Figure 6.7. The plots show that the general trend for RQI vs. time is very similar for both pavement

types. From this data, it appears that the OGDC pavements tend to develop greater roughness early on, though long-term roughness can be expected to be very similar to that of DGBC sections. For pavements between 8 and 12 years old, the DGBC pavements were generally maintaining a smoother condition.

The analyses of the RQI data with respect to base type are complicated by the fact that the initial smoothness specifications for concrete pavements were introduced at approximately the same time as the change in base types. It is believed that the significant difference in the standard deviation of RQI within the contracts which is visible at 10 to 12 years old is related to this new smoothness specification. The specification calls for grinding of rough spots which are out of tolerance. These rough spots would have simply been left prior to the specification and would likely show up as an increase in the standard deviation of RQI along the contract length.

The annual growth rate of RQI is defined as the change in RQI over the year divided by the RQI at the beginning of the year. The plot indicates that growth rates for the OGDC sections are fairly stable over time compared to those for DGBC. However, OGDC RQI growth rates appear to be slightly higher than those of DGBC.

RQI Growth: Construction Contract Averages

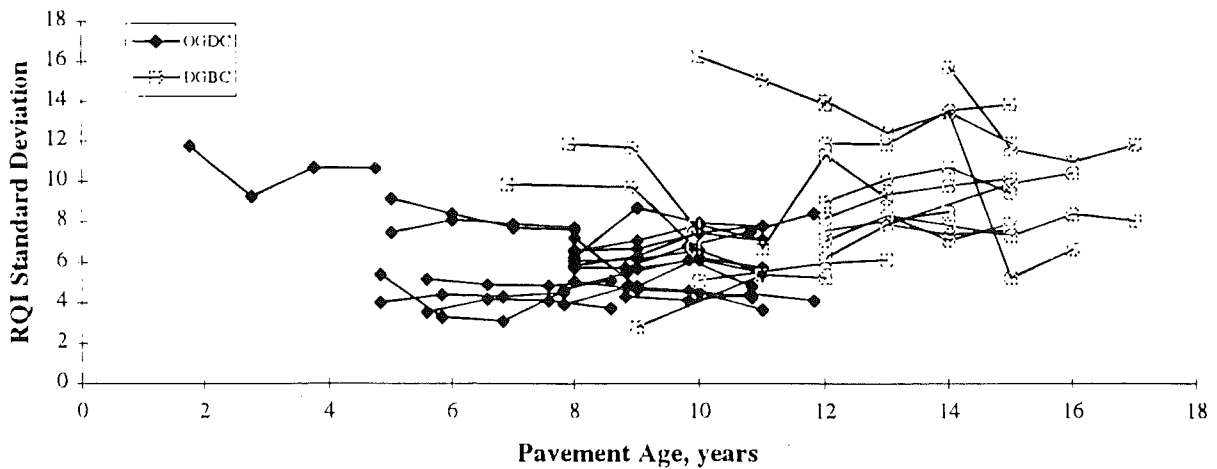
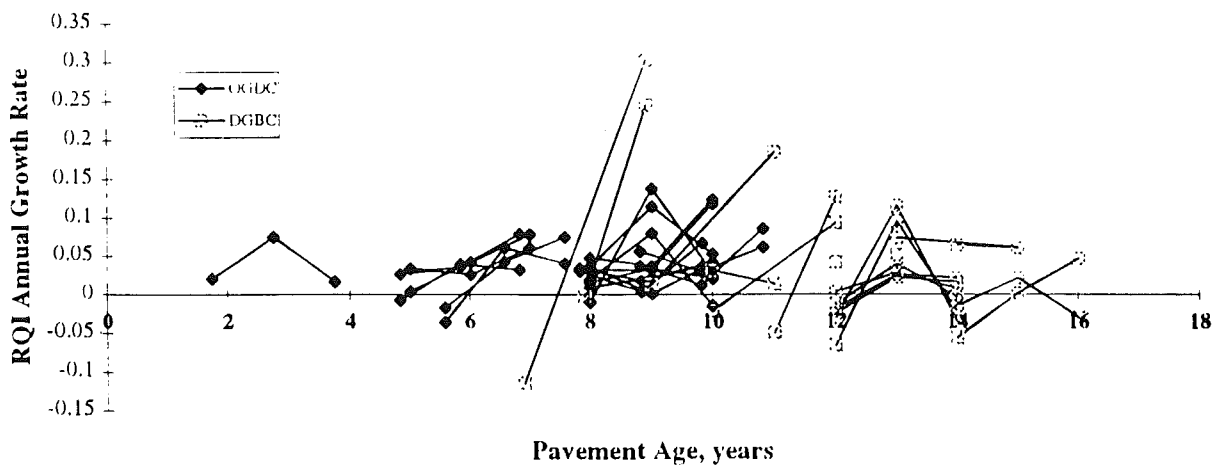
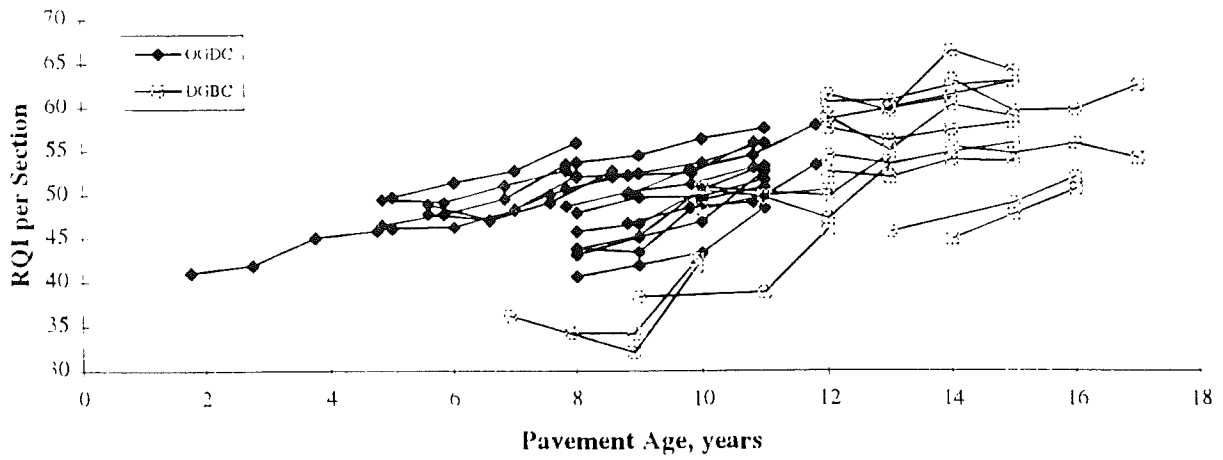


Figure 6.7 Ride Quality Index (RQI) behavior for OGDC and DGBC pavements in Michigan

7. CONCLUSIONS AND RECOMMENDATIONS

- This study has found no evidence that the OGDC base courses cause loss of support in Michigan PCC pavements as long as the OGDC consists of crushed angular material.
- The deterioration of the OGDC sections studied is in line with the LTPP GPS4 database for similar joint spacing and age. However the Watervliet sections A and C at the age of two years has a much higher than expected transverse cracking.
- Particularly for OGDC pavements it is important to avoid high temperature placements due to the increased frictional restraint during early age cooling. The relation between placement temperature of OGDC pavements and base course friction needs further study.
- During summertime construction earliest possible sawcutting is essential to relieve thermal stresses, and following FHWA recommendations for $d/3$ initial sawcut depth are suggested.
- Slab rocking has been observed for combinations of short slabs (16 ft) and high temperature placement conditions. This needs further study to determine the origin of this problem and the deterioration rate. Deterioration of 11017-32516A, section A, should be monitored since it has a large number of partial width transverse cracks starting from the longitudinal edges. It is expected that these cracks will eventually propagate to full width from repeated truck loading during morning conditions.
- A thickened subbase is recommended in cases where the subgrade has a high fines content (P200) to minimize pumping erosion of subgrade/subbase fines.
- A threshold crack width of 0.8 mm has been found to correlate well with reduced load transfer capability and occurrence of spalling. This may be a practical tool for rehabilitation assessment.
- A transverse crack frequency $L/L > 0.6$ may be considered a threshold value for need for repair.

8. REFERENCES

- *A full reference list will be added in the final report.*